Structures 33 (2021) 2839–2854

Contents lists available at ScienceDirect

Structures

journal homepage: www.elsevier.com/locate/structures

# Simplified methodologies for assessing the out-of-plane two-way bending seismic response of unreinforced brick masonry walls: lessons from recent experimental studies

S. Sharma [a], U. Tomassetti [b], F. Graziotti [c,*], G. Magenes [d]

[a] Dept. of Civil Engineering and Architecture – DICAr, University of Pavia, Italy
[b] Willis Re, London, United Kingdom (formerly DICAr, University of Pavia, Italy)
[c] Dept. of Civil Engineering and Architecture - DICAr, University of Pavia and European Centre for Training and Research in Earthquake Engineering - EUCENTRE, Pavia, Italy
[d] Dept. of Civil Engineering and Architecture - DICAr, University of Pavia and European Centre for Training and Research in Earthquake Engineering - EUCENTRE, Pavia, Italy

ARTICLE INFO

*Keywords:*
Unreinforced Masonry
Out-of-plane
Two-way Bending
Virtual Work Method
Plate Theory
Torsional Shear Strength

ABSTRACT

This paper describes a simplified methodology for the assessment of unreinforced masonry (URM) walls under out-of-plane two-way bending seismic action. The methodology involves a force-based check derived from the principle of virtual work. This check is proposed based on experimental observations of significant cracking resistance associated with two-way spanning URM walls, indicating methodologies considering such walls to be pre-cracked or to be non-laterally supported as overly conservative. The methodology incorporates several findings and developments from recent experimental campaigns: ranging from novel characterization tests on masonry couplets to incremental dynamic tests on full-scale buildings. Such incorporations include new formulation to calculate the torsional shear strength of a bed joint and accounting for possible changes in the boundary conditions of an OOP wall during dynamic loading. Testing standards as well as recommendations in several international guidelines for masonry structures addressing the input properties required to implement the proposed methodology are enlisted and reviewed. The methodology requires the definition of the period of vibration of the assessed URM walls, to calculate which plate theory based formulation is provided. Open research questions and potential avenues for further development of the methodology are ultimately highlighted.

## 1. Introduction

The out-of-plane (OOP) response of unreinforced masonry (URM) walls is a complex and ill-understood subject in the field of structural seismic analysis [1,2]. Its complexity arises from several reasons, including masonry anisotropy, structural indeterminacy of wall configurations and internal flexural stresses acting along different directions [3]. Experimentation is of paramount importance to thoroughly understand the OOP behaviour of URM and the first OOP tests on masonry walls, albeit reinforced masonry, were performed by Krauss and Vodges [4] in 1932 and Granholm [5] in 1943. However, in these experiments, failure occurred primarily in the reinforcement rather than the masonry itself. The earliest experimental studies (to the knowledge of the authors) reported in the literature on the OOP behaviour of URM were performed by Losberg and Johansson [6] in 1969. Six (3.5 m × 2 m) walls with no or varying amounts of reinforcement were tested to study the effect of varying reinforcement. Subsequent experimental work on single leaf URM walls in the OOP plane direction was performed by Satti [7] and Hendry [8] at the University of Edinburgh in 1972. A total of nineteen scaled (scale factor of 1/6) walls were tested with all edges simply-supported (6 of the 19) as well as the top edge left unsupported (13 of the 19). Also, nineteen more scaled (scale factor of 1/6) panels were tested by Kheir [9] in 1975, of which eight had all edges simply-supported and thirteen had the top edge free. OOP experiments on URM cavity walls with all four edges simply supported were also conducted by Hallquist [10] in 1970. Six full-scale single-leaf concrete blockwork walls were then tested by Anderson [11] in 1976. Though all tested walls were restrained on three edges and had their top edge kept

* Corresponding author.
*E-mail addresses:* satyadhrik.sharma@unipv.it (S. Sharma), umberto.tomassetti@willistowerswatson.com (U. Tomassetti), francesco.graziotti@unipv.it (F. Graziotti), guido.magenes@unipv.it (G. Magenes).

https://doi.org/10.1016/j.istruc.2021.03.121
Received 4 November 2020; Received in revised form 24 March 2021; Accepted 30 March 2021
Available online 23 June 2021

free, Anderson explored the effects of block thickness as well as having simple vs. continuous support along the restrained vertical edges.

Significant progress between 1977 and 1986 was also made by a dedicated experimental campaign by the British Ceramic Research Association: testing over two hundred walls under OOP two-way bending as well as one-way bending configurations in clay and calcium silicate brickwork as well as concrete aggregate blockwork masonry [12,13,14,15,16,17]. Lawrence tested thirty two clay brick URM panels in two configurations: restrained on all four edges as well as restrained on three and free on top in 1983 [18]. Anderson in 1985 again tested nine URM panels in both clay and concrete block masonry restrained on only three edges, including for the first time an experiment in which a wall which was free along a vertical edge instead of the top horizontal edge [19]. Loading was also varied between uniform lateral loading as well as edge loading. Seven walls restrained on all four edges, again in both clay brick and concrete block masonry were tested by Gairns and Scrivener in 1987 [20]. Southcombe and Tapp tested five clay brick masonry panels with openings, three edges restrained and the top edge free [21]. Candy *et al.* [22] tested nine URM walls in clay brick and well as concrete block masonry in 1989. While eight of these walls were restrained on three edges with the top edge kept free, for the first time a wall was also tested with an adjacent vertical and horizontal edge free. Chong [23] tested sixteen walls in both clay brick as well as concrete block masonry with the tested walls being restrained on all four edges, three edges or two adjacent edges. A majority of the tested walls (11 out of 16) had openings. eight scaled (scale factor of 1/2) URM infill panels in both clay and concrete blockwork masonry restrained on all four edges were tested by Abrams *et al.* [24].

Most of the works (other than Abrams *et al.* [24]) mentioned until now were performed in the context of wind resistance rather than the seismic resistance of URM. Also, loading was static and monotonic, applied in most cases by increasingly inflating an airbag till failure of the specimen was reached, which cannot well represent the dynamic cyclic loading of a real earthquake scenario. Nevertheless, such studies established that under OOP loading in a two-way bending configuration, URM walls fail in patterns very similar to concrete slabs and that this similarity is limited only to the geometry of the failure patterns owing to the "brittle" nature of masonry as a material [25]. Seismic behaviour is better studied by administering load reversals as in a real earthquake scenario and can be achieved by both quasi-static cyclic tests as well as dynamic tests. Quasistatic cyclic tests which involve applying a load pattern typically at a slow loading rate (as compared to dynamic tests) afford better testing control and consequently a better characterisation of its load–displacement behaviour. In contrast, dynamic testing involves subjecting the test specimen to acceleration histories and allows the recreation of a real earthquake scenario. For a more detailed discussion on a comparison of the response of URM when subjected to different testing methods (which is not the focus of this review) a reader is referred to Calvi *et al.* [26] and Graziotti *et al.* [27].

A distinct majority of experimental studies on the seismic response of URM structures have focussed on the primary load transfer path of seismic forces in a URM structure *i.e.* the in-plane direction of walls (including but not limited to [28,29,30,31]). While research on the OOP behaviour of URM is limited, this limited work also has been primarily on one-way spanning URM panels (with no lateral edges supported). Here it is important to distinguish explicitly among two types of OOP response of URM walls *i.e.* the one-way bending case occurring in walls with only horizontal or vertical edges restrained and the two-way bending case in walls with both horizontal and vertical edges restrained. Griffith *et al.* [32] tested fourteen one-way spanning walls, subjecting them to both static as well as dynamic excitation. Simisir *et al.* [33] tested more one-way spanning walls dynamically taking into account the effects of flexible floor diaphragms. Advances in the shake table testing of one-way spanning walls have also been made by Penner and Elwood [34], Giaretton *et al.* [35] and most recently by Graziotti *et al.* [36] who performed incremental dynamic tests on one-way spanning single leaf and cavity walls.

As regards, experimental studies on the OOP two-way bending seismic response of URM panels, Restrepo-Vélez *et al.* [37] (scale factor of 1/5) performed inclined table tests while Vaculik *et al.* [38] (scale factor of 1/2) carried out airbag tests on scaled dry stack masonry walls. Monotonic followed by cyclic loading of eight full-scale mortared walls was carried out by Griffith *et al.* [39]. Walls were tested in a large array of boundary conditions and considerations were adopted also to account for the presence of openings and vertical overburden. Walls in the same configuration, albeit scaled (scale factor of 1/2) were also tested dynamically by Vaculik and Griffith [40]. Five single-leaf walls (considering different unit-mortar combinations) were also tested under quasi-static cyclic loading by Messali et al. [41] and Damiola *et al.* [42]. Four scaled single leaf rubble-stone walls (scale factor of 1/2) were also tested by Maccarini *et al.* [43]. Additionally, in-situ quasi-static airbag tests were also performed by Walsh *et al.* [44] on walls in an existing building. A single full-scale mortared URM wall (among others retrofitted with composite materials) was also tested under cyclic loading by Padalu *et al.* [45].

The review provided above clearly indicates that what had been critically missing from literature are dynamic experiments considering seismic loading on full-scale URM panels in a two-way bending configuration. Such a shortcoming was addressed in works by the authors *i.e.* Graziotti *et al.* [46] and Sharma *et al.* [47] who performed incremental dynamic shaking table tests on full-scale URM panels in a two-way bending configuration. While a plethora of numerical strategies (including but not limited to [48,49,50,51,52,53,54,55,56]), can be found in the literature for the structural analysis of URM structures [57] and have also been demonstrated to be able to adequately capture the OOP response of URM, the performance of such strategies depend highly on user skill, available computational resources as well as the precise knowledge of material properties [58]. Consequently, design rules and analytical methods because of their simplicity and ease of use are still the most widely and commonly utilised methods in engineering practice. Considering this, observations from these state-of-the-art experimental campaigns *i.e.* Graziotti *et al.* [46] and Sharma *et al.* [47] are used to provide a discussion in this paper on which design rules, analytical methods and their associated assumptions/simplifications seem to be more appropriate for performing simplified assessment of URM walls under OOP two-way bending seismic excitation. The discussion presented can also support amendments of existing codes and guidelines for the design and assessment of unreinforced masonry structures. Limitations of the state-of-the-art analytical methods, which warrant further research attention are also identified and enlisted at the end of the provided discussion.

A majority of current international standards addressing masonry structures either do not account for the effects of URM walls having both horizontal and vertical edges supported *i.e.* treat two-way bending as one-way bending or have conceptual flaws associated with how they account for two-way bending behaviour. Standards currently accounting for OOP two-way bending behaviour are: Eurocode 6 [59], the Australian standard for masonry structures: AS 3700 [60] and the Canadian code for masonry structures: CSA S304-14 [61]. They all provide analytical formulation, based on improved versions of yield line analysis developed originally for reinforced concrete slabs by Johansen [62], for calculating the two-way bending strength of URM walls. This was based on the similarity of failure mechanisms between two-way spanning reinforced concrete slabs and URM walls as observed by early experimental studies [25]. The yield line method requires the knowledge of the failure mechanism *a priori* and assumes capacities along all cracks to have reached simultaneously. Eurocode 6 still uses the yield line method [59] while the Canadian code for masonry structures [61] uses a modified form of it: the fracture line method developed by Drysdale and Baker [63] which neglects the contribution of horizontal and central vertical cracks. In this context, it is also important to mention the fracture line method developed by Sinha [64,65] who modified the yield

line method to take into account the material orthotropy of URM. The Australian standard [60] instead uses an approach developed by Lawrence and Marshall [66], based on the virtual work method which similar to the fracture line method, also ignores the contribution from horizontal cracks but also assumes the slope of diagonal cracks to be based on the geometry of masonry units. A major improvement of this method was carried out by Willis [67] in his doctoral thesis (also reported in [68,69]), where he developed mechanical equations for calculating moment capacities associated with horizontal and diagonal cracks, departing from the empirical formulation that is still implemented in the Australian code [60]. An improvement of these expressions was also carried out by Vaculik [70] and this method forms the state-of-the-art of design rules available to calculate the strength of URM wall panels in OOP two-way bending. For a detailed review of all these analytical methods and their underlying assumptions and limitations, the reader is referred to the doctoral thesis of Vaculik [70] while a quantitative comparison of their performance can be found in Maluf *et al.* [71] and Chang *et al.* [72].

Guidelines not accounting for two-way bending behaviour of URM walls include the C-8 (2018) [73] of New Zealand. C-8 (2018) includes only the non-linear kinematic analysis (NLKA) method for the out-of-plane assessment of unreinforced masonry walls. The NLKA method implicitly assumes an initial cracked state of the wall being assessed, given that the associated calculations are inapplicable for un-cracked walls. Such an assumption (*i.e.* to consider the wall to be in an initial cracked state) can be considered conservative for vertically spanning walls (with no lateral edges supported) exhibiting one-way vertical bending behaviour, where the initial cracking resistance (controlled by the bond strength of masonry) in a majority of cases is significantly lower than the force required to trigger the kinematic mechanism. It is also interesting to note that guidelines for masonry structures in the USA *i.e.* TMS 402–11/ACI 530–11/ASCE 5–11 and TMS 602–11/ACI 530.1–11/ASCE 6–11 (2011) [74] also treat two-way spanning walls as one-way spanning walls.

In this paper, the proposed simplified methodology for assessing URM walls under two-way bending is first presented in section 2. Primary calculations involved in the methodology are described in section 3. Additional special checks, accounting for more observations made during the incremental dynamic testing of walls with openings and cavity walls in as well as the out-of-plane collapse of walls in full-scale buildings tested dynamically are provided in section 3.1. Testing procedures to experimentally evaluate and recommendations present for the input material parameters in standards are summarised in section 4. Charts to evaluate the period associated with the fundamental mode of vibration of two-way spanning URM walls are then provided in section 5. A step-by-step summary of the methodology is then provided in section 6. The performance of the proposed methodology against full-scale dynamic experimental results is then presented in section 7, tabulating also all the details required to perform analytical modelling of the experimentally tested walls. Limitations and potential avenues of improvement of the state-of-the-art analytical methods are ultimately highlighted in section 8.

## 2. Proposed methodology

For one-way spanning URM walls, the OOP cracking resistance is controlled by the bond strength of masonry [75,76] and is often lower than the force required to trigger a kinematic mechanism. Consequently, assuming an initial cracked state can be considered reasonable while assessing such walls. However, in the case of two-way spanning URM walls, evidence from recent experimental studies: Graziotti *et al.* [46] and Sharma *et al.* [47] indicate that such an assumption, *i.e.* treating two-way walls as one-way and considering them to be in an already cracked state, can be overly conservative. Nine full-scale URM walls were tested under incremental dynamic seismic action and all the tested panels showed peak cracking resistance significantly higher than the force associated with any kinematic mechanism. For two-way spanning walls, the simplified methodology proposed in this paper accounts for this higher cracking resistance (compared to one-way walls) through an elastic force-based check based on the Virtual Work Method (VWM) to calculate their peak cracking resistance (*PCR*). This calculations of *PCR* proposed here have been evaluated to show good agreement with experimental evidence in several studies [46,47,39,77]. The *PCR* is to be compared directly with the seismic demand (Fig. 1).

On the exceedance of *PCR*, it can be observed in Fig. 1, that non-linear kinematic analysis (NLKA) methods [78,79] (also present in C-8 (2018) [73]) which do not consider the presence of cracked lateral supports (*i.e.* assume a one-way bending configuration) are proposed to be safely used while performing simplified assessments. This is not only a conservative assumption but also based on what was experimentally observed for several Weak Unit-Strong Joint URM [47] walls in both reference experimental studies [46,47]. In this context, Weak-Unit Strong Joint URM refers to masonry which exhibits line failure (see equation (2) in section 3) passing through masonry units and head joints under pure horizontal bending. As can be expected, such walls exhibit line failure at their lateral supports also once *PCR* has been exceeded and consequently exhibit a pure one-way bending behaviour (Fig. 2). The methodology automatically considers the tendency of long two-way spanning walls with supported vertical edges far apart from each other to behave in OOP one-way bending.

While the recommendation to consider pure one-way bending on the exceedance of *PCR* is conservative and can be considered appropriate for simplified methodologies such as the one proposed by this paper, the post-*PCR* behaviour of two-way spanning URM walls depends on the exact nature of cracks separating the wall and its lateral supports. Instead of pure line failure as observed in the reference experimental campaigns, stepped failure or as noted by Vaculik and Griffith [80] also a mix of line and stepped failure may occur at such connections. Despite having received relatively limited attention in the existing literature, to consider the post-PCR two-way bending behaviour of URM walls, an interested reader is referred to Vaculik and Griffith [81] and Padalu *et al.* [82].

Seismic force-reduction factors (the so-called $q$ or $R$ factor), are generally used in codes to reduce the elastic design spectrum ordinates when using linear assessment procedures for structures and elements with non-negligible ductility capacity [83]. The brittle behaviour observed for Weak Unit-Strong Joint URM specimens in the reference experimental studies [46,47] indicated extremely limited ductility capacity and suggests not to use any reduction factors for these elements (*i.e.* $R = 1$). Strong Unit-Weak Joint URM specimens, exhibiting stepped failure (see equation (2) in section 3) passing through head and bed joints under pure horizontal bending, were characterized by a relatively higher ductility capacity. Preliminary studies adopting a nonlinear dynamic single-degree-of-freedom model calibrated to the reference experimental campaign data [84] indicate larger but still limited values for such elements. For these reasons, the suggestion is to not apply any reduction factors, at least before extensive parametric numerical analyses are performed to calculate them.

## 3. Calculation of the peak cracking resistance (*PCR*)

The primary term that has to be calculated in the proposed methodology is *PCR i.e.* the peak cracking resistance associated with two-way spanning URM walls. To compute *PCR*, a codified form of the virtual work method developed by Lawrence and Marshall [66] and already implemented in the Australian standard for designing masonry structures *i.e.* [9] is to be used. Important assumptions inherent in the method are that moment capacities of all diagonal and horizontal cracks are reached simultaneously and the resistance provided by horizontal cracks to peak strength is neglected. The method preselects a failure mechanism (Fig. 3) for the assessed wall based on its geometry and boundary conditions, calculating the *PCR* associated with the failure mechanism as

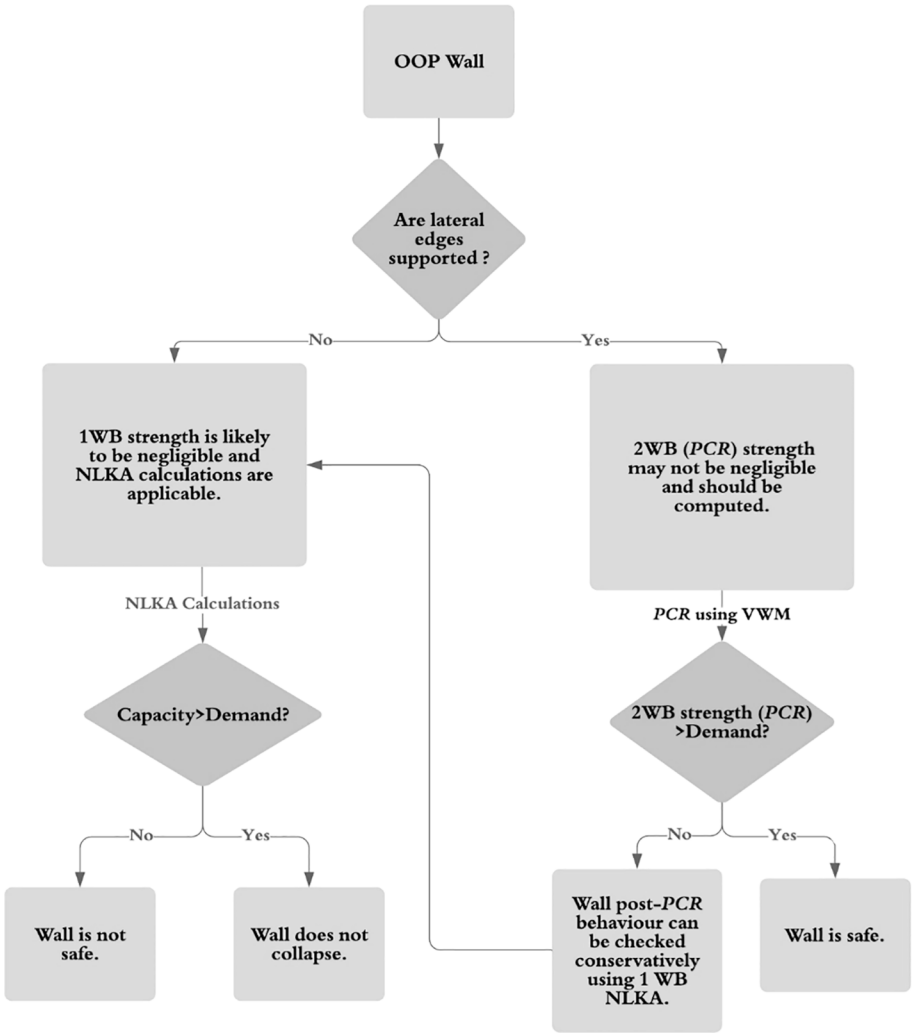


**Fig. 1.** Flowchart explaining the proposed methodology for the out-of-plane assessment of two-way spanning URM walls.

per equation (1):

$$PCR = \frac{2a_f}{g \times L_d^2}(k_1 M_h + k_2 M_d) \times L \times H \tag{1}$$

where

*PCR* is the peak cracking resistance, normalised with respect to *g* (*g* is the acceleration due to gravity = 9.81 m/s$^2$);

$a_f$ is the aspect factor calculated as per Table 1;

*k1*, *k2* are coefficients calculated as per Table 1;

*L*, *H* are the length and height respectively of the wall panel being assessed;

$L_d$ is the design length calculated as: (i) the actual length of the wall to the unsupported end, when only one vertical edge of the wall is laterally supported; (ii) half the actual length of the wall between lateral supports, when both vertical edges are laterally supported; (iii) the distance from the laterally supported end of the wall to the nearest edge of the opening, when an opening is present in the wall (see Fig. 4);

The codified form of the virtual work method already implemented in the Australian standard for designing masonry structures *i.e.* [9] is however improved for what concerns the equations used for computing the horizontal ($M_h$) and diagonal ($M_d$) bending moment capacity of unreinforced masonry *i.e.* equations (2) and (3). The equations currently recommended to be used in [9] are empirical and state-of-the-art analytical equations developed by Willis [67] and Vaculik [70] are proposed to be used instead. In equation (1), $M_h$ is the horizontal bending moment capacity per unit crack length calculated as per equation (2):

$$M_h = lesser\ of \begin{cases} \dfrac{1}{2(h_u + t_j)}\left[(f_{ut} - \nu \cdot \sigma) \cdot h_u \dfrac{t_u^2}{6}\right] (Weak\ Unit - Strong\ Joint/Line\ failure) \\ \dfrac{1}{h_u + t_j}\left[\tau_u \cdot k_b \cdot 0.5 \cdot (l_u + t_j) \cdot t_u^2\right] (Strong\ Unit - Weak\ Joint/Stepped\ failure) \end{cases} \tag{2}$$

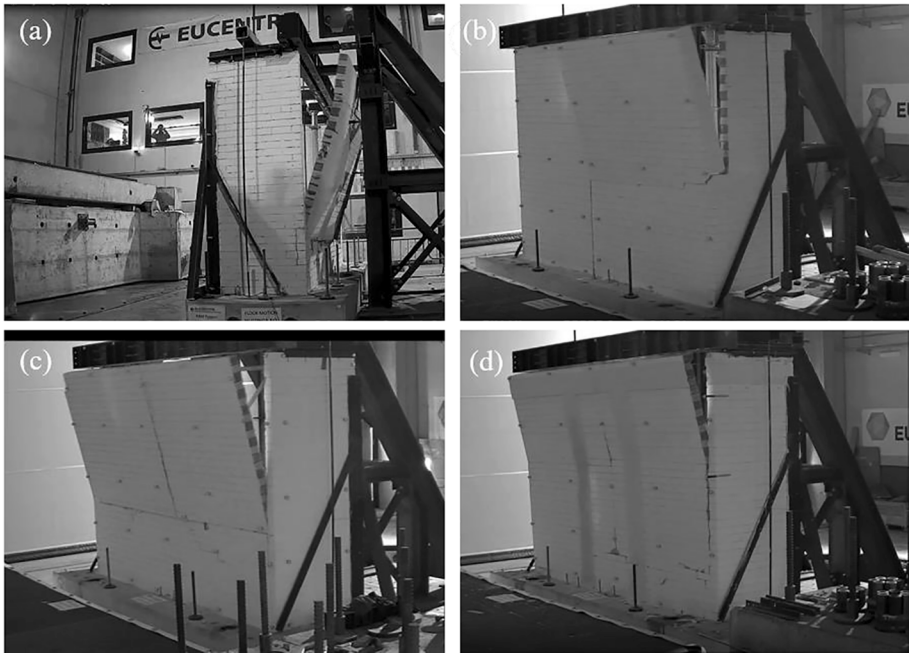


**Fig. 2.** One-way bending behaviour experimentally observed for Weak Unit-Strong Joint (line failure) URM walls after the exceedance of their peak cracking resistance (*PCR*): (a) wall CS-000-RF in Graziotti *et al.* [46]; (b) CS-000-L2; (c) CS-000-RFV and (d) CS-000-RF2 in Sharma *et al.* [47].

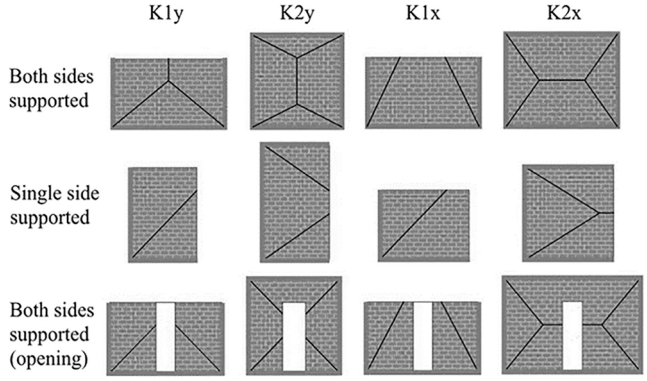


**Fig. 3.** Failure mechanisms preselected by the virtual work method based formulation [66] under out-of-plane two-way bending based on wall geometry and boundary conditions (reproduced from [70]).

and, $M_d$ is the diagonal bending moment capacity per unit crack length calculated as per equation (3):

$$M_d = \frac{\sin\varphi}{h_u + t_j}\left[(\sin\varphi)^3 \cdot \tau_u \cdot k_b \cdot 0.5 \cdot (l_u + t_j) \cdot {t_u}^2 + (\cos\varphi)^3 \cdot (f_{mt} + \sigma) \cdot \frac{0.5 \cdot (l_u + t_j) \cdot {t_u}^2}{6}\right] \quad (3)$$

In equations (2) and (3):

$l_u$, $h_u$ and $t_u$ are the length, height, and thickness of a brick unit (Fig. 5);

$t_j$ is the thickness of a mortar joint (Fig. 5);

$\varphi$ is the assumed slope of a diagonal crack calculated from unit geometry as $2(h_u + t_j)/(l_u + t_j)$, an inherent assumption of the proposed calculations is that the diagonal cracks follow the natural diagonal slope of masonry *i.e.* one bed joint across, one perpend joint up and so on (Fig. 5);

$f_{mt}$ is the flexural tensile strength of masonry as a composite obtained from the bond wrench test;

$f_{ut}$ the flexural tensile strength of a brick unit;

**Table 1**
Coefficients required to calculate *PCR* associated with two-way spanning walls as per equation (1) (reproduced from [60]).

| *Op.* | *NVE* | *α[-]* | $\alpha_f$[-] | $k_1$[-] | $k_2$[-] | Mechanism (Fig. 3) |
|---|---|---|---|---|---|---|
| No | 2 | ≤1 | $\frac{1}{\left(1-\frac{\alpha}{3}\right)}$ | $\frac{R_{f1}+R_{f2}}{2}+1-\alpha$ | $\alpha\left(1+\frac{1}{{G_n}^2}\right)$ | K2Y |
| No | 2 | >1 | $\frac{\alpha}{\left(1-\frac{1}{3\alpha}\right)}$ | $\frac{R_{f1}+R_{f2}}{2}$ | $1+\frac{1}{{G_n}^2}$ | K2X |
| No | 1 | ≤1 | $\frac{1}{\left(1-\frac{\alpha}{3}\right)}$ | $R_{f1}$ | $\alpha\left(1+\frac{1}{{G_n}^2}\right)$ | K1Y |
| No | 1 | >1 | $\frac{\alpha}{\left(1-\frac{1}{3\alpha}\right)}$ | $R_{f1}$ | $1+\frac{1}{{G_n}^2}$ | K1X |
| Yes | 2 | ≤1 | $\frac{1}{\left(1-\frac{\alpha}{3}\right)+\left(1-\frac{\alpha}{2}\right)\frac{l_o}{l_d}}$ | $R_{f1}$ | $\alpha\left(1+\frac{1}{{G_n}^2}\right)$ | K2Y |
| Yes | 2 | >1 | $\frac{\alpha}{\left(1-\frac{1}{3\alpha}\right)+\frac{l_o}{2l_d}}$ | $R_{f1}$ | $1+\frac{1}{{G_n}^2}$ | K2X |

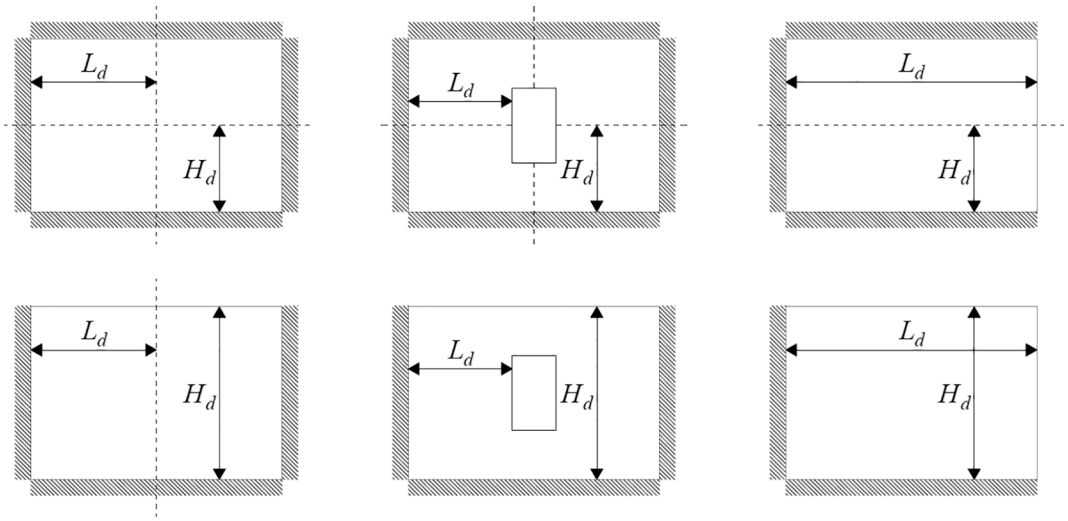


**Fig. 4.** $L_d$ and $H_d$ for two-way spanning walls with varying support configurations and in the presence/absence of openings.

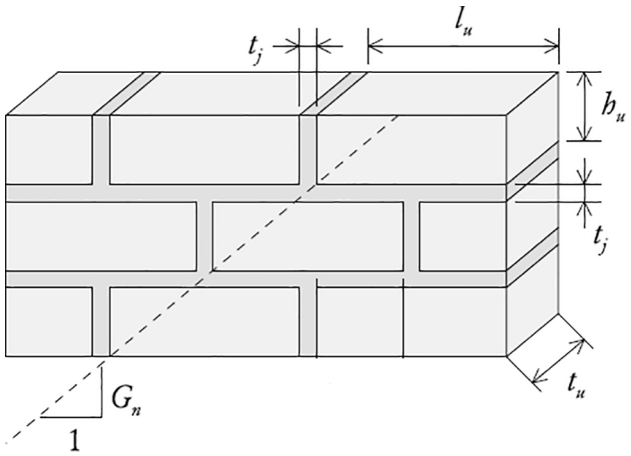


**Fig. 5.** Notation related to basic geometrical properties required for the calculation of *PCR* (reproduced from [70]).

σ is the vertical pre-compression at mid-height of the wall;

$\nu$ is the Poisson's ratio of masonry which can be taken as 0.2;

$\tau_u$ denotes the torsional shear strength of a masonry bed joint which can be calculated as per two different approaches as per recommendations presented in section 4.3;

and $k_b$ is a numerical constant whose value which depends on the approach adopted to calculate $\tau_u$ and is described in more detail in section 4.3

In Table 1:

$G_n$ (has the same value as $\varphi$) and is calculated as $2(h_u + t_j)/(l_u + t_j)$ (Fig. 5);

$\alpha$ is a slope factor calculated as $G_n L_d/H_d$ controlling the association of K1X or K1Y mechanisms with $\alpha = 1$ being the limiting case between the complementary X and Y mechanisms;

$R_{f1}$ and $R_{f2}$ are restraint factors for the first and second (if any) supported edges of the wall, respectively. These factors assume a value of 0 if no rotational restraint is present (*i.e.* simply supported), a value of 1 if the supported edge is fully restrained against rotation (*i.e.* fully fixed) and intermediate values in case of partial rotational restraint. Validation of the proposed methodology to calculate *PCR* against the experimental studies can be found in [46,47,39,77], showing good agreement when a value of 0.5 is adopted which is the recommended value to be adopted while performing the assessment.

### 3.1. Special considerations

This section of the paper provides special considerations that should be taken into account while assessing walls with openings and cavity walls. An additional check, accounting for the possible loss of restraint during an earthquake along the top edge of a wall is also provided. These proposed considerations are based on experimental observations either in the reference testing campaigns [46,47] or in case of section 3.1.3, the OOP two-way bending collapse of a wall during the incremental dynamic testing of a full-scale building [85].

#### 3.1.1. Walls with large openings

In the case of walls with large (opening occupying at least 25% of the total wall face area) openings, an alternative configuration for the calculation of *PCR* can be that of considering only the larger of the two panels on either side of the opening (with the opening edge assumed to be free), as indicated in Fig. 6. Though not necessarily conservative, this configuration gave a better estimation of *PCR* for the wall with an opening tested dynamically in Graziotti *et al.* [46].

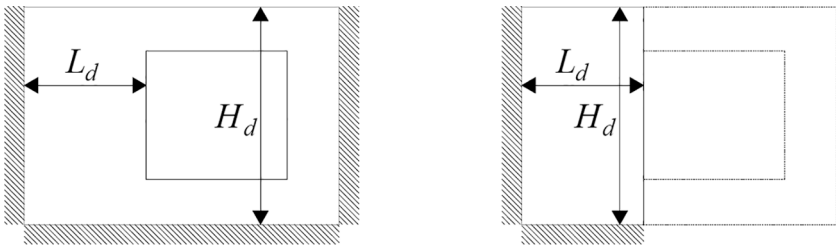


**Fig. 6.** Normal configuration (right) and additional special configuration (left) to be considered in case of walls with openings.

### 3.1.2. Cavity walls

For cavity walls, the *PCR* has to be first evaluated for the constituent leaves individually. If the horizontal displacement compatibility (even if the ties are flexible) of the two leaves can be ensured and the pull-out force of the entire tie-wall system as well as the axial capacity of the ties is higher than the *PCR* of the stronger constituent leaf, the two leaves can be considered to be acting together. In the reference experimental campaign, this was ensured by steel ties at a spacing of 2 ties/m$^2$. In such a case, the *PCR* of the cavity wall is to be taken as the sum of the *PCR* of the individual leaves and the period (see section 5) to be considered for such a wall is of the leaf corresponding to a higher acceleration demand. However, when the combined behaviour of the two leaves cannot be ensured, the *PCR* of the cavity walls is recommended to be taken as the lower among the two leaves.

### 3.1.3. Possible loss of restraint along the top edge of walls during an earthquake

Tomassetti *et al.* [85] demonstrated the possibility of a loss of restraint along the top edge of a wall during an earthquake in the absence of mechanical connectors. This failure was induced by the pronounced rocking mechanism developed by the slender longitudinal piers combined with the applied vertical input motion which led to an uplift of the RC slab causing a loss of restraint at the top of the out-of-plane wall, rendering it much more vulnerable to out-of-plane actions (*i.e.* reduced *PCR*). This loss of restraint ultimately led to its out-of-plane two-way bending collapse (Fig. 7). Similar observations in terms of loss of restraint along the top edge of OOP walls being provoked by the in-plane rocking of adjacent perpendicular walls have also been made in shaking table tests performed by Beyer *et al.* [86] on a mixed Reinforced Concrete/URM building and Senaldi *et al.* [87] on stone masonry buildings.

Such experimental evidence underlines the importance of considering potential variations of wall boundary conditions, especially restraint conditions along the top edge of walls. A wall initially restrained on both vertical and horizontal edges might have to be considered free on top (which effectively implies that in the case of vertically spanning walls restrained at the top, such a wall might be subjected to just simple overturning during an earthquake). Indeed, for out-of-plane walls having a top restraint and adjacent in-plane wall piers that are deemed as being capable of causing uplift of the slab, the out-of-plane wall being assessed can be considered to be retrained on the top only if the deflection of the supported slab is at least equal to that of the uplift induced by the in-plane piers. Special attention needs to be placed to this check in presence of specific mechanical connectors or retrofit measures that may inhibit the uplift of the floor or the loss of restraint (*i.e.* [88]).

A check is therefore proposed to take into account such variation of boundary conditions that might occur during the earthquake. It is to be noted that this check needs to be performed only in the presence of floor diaphragms corresponding to structural systems that are capable of causing uplift of the portion of the structure above the assessed wall, as in the case of two-way spanning slabs or slabs spanning only in the direction parallel to the length of the assessed wall. If the vertical deflection caused by the overburden load of such a slab is lower than the uplift caused by the longitudinal piers, the top edge of the wall below the slab can no longer be assumed to be effectively restrained (Fig. 7 and Fig. 8). To account for this, the proposed check consists of initially evaluating the stiffness *(EI)* of a strip of unit width of the floor system parallel to the wall, idealising this strip to be a uniformly loaded simply supported beam and equating its maximum deflection to the uplift caused by drift of the in-plane piers as per equation (4):

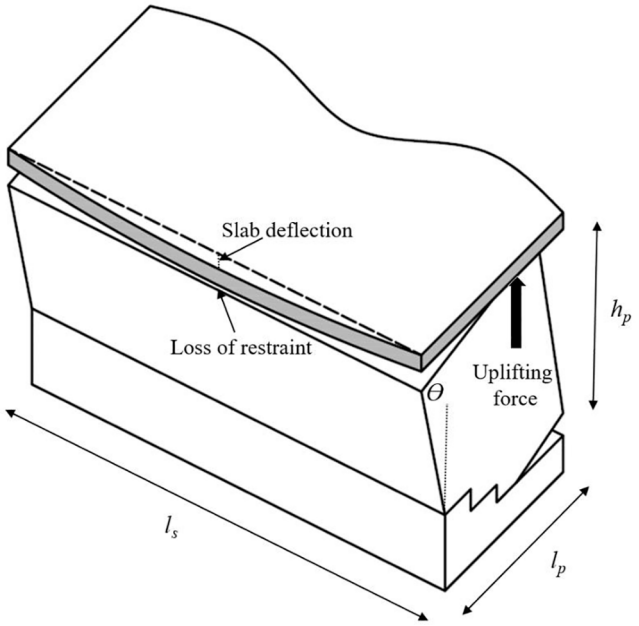


**Fig. 8.** Notation related to basic geometrical properties required to check for a possible loss of restraint along the top edge of URM walls during an earthquake [90].

$$EI = \frac{5 \times q \times l_s^4}{384 \times \theta \times l_p} \tag{4}$$

where $q$ is the load per unit length and unit width of the floor system parallel to the wall;

$l_s$ is the span length of the floor system in the transverse direction (perpendicular to the out-of-plane direction of the wall being assessed) (Fig. 8);

"Θis the drift demand of longitudinal piers. For demonstrating a graphical way of performing this check, charts are provided in Fig. 9 adopting Θ = 1.25%. This value can be considered an reasonable upperbound value of drifts in codes associated with the in-plane rocking/flexural failure capacity of URM piers. However, even higher values can be found in literature: an average ultimate drift capacity of 1.73%

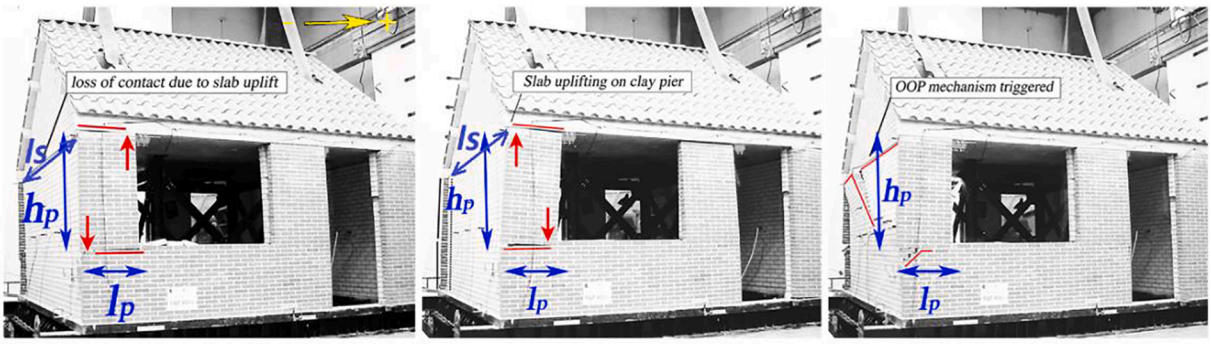


**Fig. 7.** Progressive development of out-of-plane two-way bending collapse of a wall due to loss of top restraint [85].

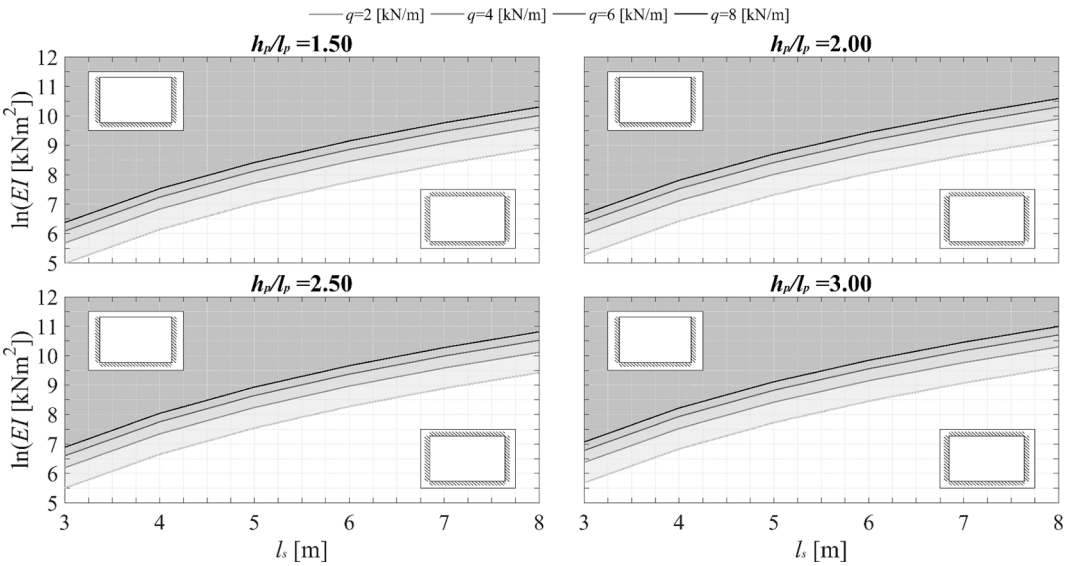


**Fig. 9.** Charts for assessing restraint at the top edge of URM walls as a function of the geometry and stiffness of the floor system (plotted for Θ = 1.25%).

was calculated from an extensive experimental dataset (corresponding to 38 experiments) by Messali and Rots [89]. To account for such drifts, similar charts can be developed (for any value of required by the code or the Θengineer) by simply adopting equation (4) and the explanation provided along with Fig. 9;"

$l_p$ is the effective length of the longitudinal pier (Fig. 8).

If no mechanical connectors are present, a simplified way of analysing the possible loss of restraint along the top edge of the walls is provided in terms of the charts given in Fig. 9. Four different charts are provided for longitudinal piers of aspect ratios $h_p/l_p$ ranging from 1.5 to 3.0, adopting a drift demand of Θ = 1.25%. With *EI* calculated using equation 8 and span length $l_s$ controlling the ordinate and abscissa respectively, the location of the calculated point above a curve provided for the acting *q* indicates that the deflection of the slab is lower than the uplift induced by the longitudinal piers, and thus the top edge of the wall cannot be considered as restrained. To facilitate the visibility of the charts, natural logarithm of the values of *EI* are plotted. Conversely, a calculated point located below a curve provided for the acting *q* indicates that the slab is flexible enough to ensure some connection between the slab and wall and thus the top edge of the wall can be considered as restrained. In case of floor slabs spanning exclusively in the direction perpendicular to the length of the assessed wall, this check does not need to be performed and the wall can be considered restrained on all four edges, since the slab is laid on the wall itself.

## 4. Material properties

The proposed methodology requires the explicit definition of three specific material mechanical properties: the flexural tensile strength of a brick unit ($f_{ut}$), the flexural tensile strength of masonry as a composite obtained from the bond-wrench test ($f_{mt}$) and the torsional shear strength of a masonry bed joint ($\tau_u$). Recommendations for $f_{ut}$ and $f_{mt}$ present in various guidelines are highlighted. Standardised testing procedures available to experimentally evaluate parameters $f_{ut}$ and $f_{mt}$ are also enlisted. For $\tau_u$, a formula developed by Sharma *et al.* [91] is described along with other empirical approaches present in literature, which correlate $\tau_u$ with $f_{mt}$ The methodology [91] instead calculates $\tau_u$ based on values of $f_{v0}$ and $\mu$ *i.e.* cohesion and friction coefficient. Standardized procedures to estimate $f_{v0}$ and $\mu$ experimentally as well as recommendations in various guidelines are also addressed.

### 4.1. Flexural tensile strength of a brick unit ($f_{ut}$)

The flexural tensile strength of a brick unit can be evaluated experimentally as per the recommendations of RILEM TC. LUMA2 [92], ASTM C1006-07 [93] or AS/NZS 4456.15 [94]. No European standard currently addresses a procedure to evaluate $f_{ut}$. However, Eurocode-8 (1998) [95] currently has clauses recommending the calculation of $f_{ut}$ based on $f_u$ *i.e.* the normalized mean compressive strength of the brick units in the direction of the applied action effect. $f_u$ can be evaluated experimentally based on recommendations in EN 772–1 [96], RILEM TC. LUMA1 [97], ASTM C140/C140M-20 [98] and AS/NZS 4456.4 [99].

Specifically, clause C.4.3.1 of Part 3 of Eurocode-8 (1998) [95] recommends assuming $f_{ut}$ as 6.5% of $f_u$. This assumption *i.e.* calculating $f_{ut}$ based on $f_u$ was compared against experimental investigations of the same parameter in several experimental studies [46,47,100,101,102]. It was gathered that for the case of solid Calcium Silicate units $f_{ut}$ can be conservatively assumed as 10% of $f_u$ while for solid clay units the proposal found Eurocode-8 [95], *i.e.* $f_{ut}$ equal to 6.5% of $f_u$, appears to be more appropriate. Clause C8.7.2 of C-8 (2018) [73] calculates both the probable (as this particular guideline addresses the assessment of existing buildings) compressive strength and tensile strength of brick units based on their hardness characteristics based on the recommendations of Almesfer *et al.* [103] in clause C8.7.2. The hardness characteristics, in turn, are established by scratching the surface of bricks with different objects. Guidelines for masonry structures in the USA *i.e.* TMS 402–11/ACI 530–11/ASCE 5–11 and TMS 602–11/ACI 530.1–11/ASCE 6–11 (2011) [74] make no explicit recommendations for the values of the flexural tensile strength of masonry units. It can, however, be implicitly understood that the use of ASTM C1006-07 [93] to establish the splitting tensile strength of masonry units is recommended. AS 3700 (2018) [60]) also recommends testing as per AS/NZS 4456.15 [94] to obtain the value of $f_{ut}$, not allowing values higher than 0.8 MPa unless justified by testing while performing the out-of-plane assessment of URM walls.

### 4.2. Flexural tensile strength of brick masonry ($f_{mt}$)

The flexural tensile strength of masonry as a composite can be evaluated experimentally with the help of the bond-wrench test performed as per the recommendations of EN 1052–5 [75], RILEM TC. LUMB2 [76] or Appendix D of AS 3700 (2018)[60]. Eurocode 6 (2006) [59] provides values of flexural tensile strength for different types of masonry in Clause D.2 of Annex D. C-8 (2018) [73] recommends

adopting the tensile strength of URM to be zero unless the assessed walls show no signs of cracking and in-plane calculations indicate cracking of brickwork is not expected. TMS 402–11/ACI 530–11/ASCE 5–11 and TMS 602–11/ACI 530.1–11/ASCE 6–11 (2011) [74] also neglects the tensile strength of masonry. For earthquake assessment, AS 3700 (2018) [60] recommends adopting a value of not higher than 0.20 MPa unless justified by experimental data for normal URM. In fact, for special cases/masonry, the bond-wrench test is recommended as per Appendix D of [60].

### 4.3. Torsional shear strength of a masonry bed joint ($\tau_u$)

In both equations (2) and (3), $\tau_u$ denotes the torsional shear strength of a masonry bed joint. No standardised test currently exists to estimate this parameter in the existing literature. A rational mechanics based formulation for $\tau_u$ which calculates the torsional shear strength of URM bed joints based on their $f_{v0}$: cohesion, $\mu$: friction coefficient values, evaluated from standardised direct shear tests [104,105] has been developed in Sharma *et al.* [91] and is proposed to be used. The methodology adopted to develop this formulation involved first performing experiments on masonry couplets corresponding to various brick–mortar combinations, subjecting them to torsional shear under varying levels of vertical compression. These experiments were subsequently modelled using a refined finite-element based numerical model, exhibiting good agreement with the experimental results. A simplified mathematical model taking into account these findings were then used to develop the charts provided in Fig. 11. This proposed formula takes into account a non-linear distribution of shear stresses at the attainment of peak torque resistance by choosing $k_b$ from Fig. 11 based on the value of $f_{v0}$, $\mu$, as well as the acting level of $\sigma$ while $\tau_u$, is proposed to be evaluated as $\tau_u = f_{v0} + \mu\sigma$. This analytical approach has also been shown in [91] to predict well the median values of the aforementioned experimental torsional shear tests on clay and CS masonry couplets, showing a reduced dispersion compared to the other literature approaches described in following paragraphs, when failure under torsional shear occurs at the brick–mortar interface (Fig. 10a). However, significantly higher torsional shear strength than what is calculated using the proposed formula was exhibited experimentally by masonry couplets for which failure under torsional shear was through the thickness of the mortar joint (Fig. 10b). For the same batches of masonry, failures in direct shear tests which were used to obtain input parameters of the proposed formulation were limited to the unit-mortar interface. For more information on this and how the formulation was developed, the reader is referred to Sharma *et al.* [91].

Values of $f_{v0}$ and $\mu$ can be evaluated experimentally by the direct shear test on masonry triplets as per the recommendations of EN 1052–3 [104]. Additionally, these quantities can be evaluated in-situ as per the recommendations of ASTM C1531-16 [105] or RILEM TC. MS.D6 [106]. Similar to the recommendations for probable compressive and tensile strength of brick units, C-8 (2018) [73] calculates both the probable cohesion and friction coefficient of masonry based on their hardness characteristics based on the recommendations of Almesfer *et al.* [103] in clause C8.7.2. TMS 402–11/ACI 530–11/ASCE 5–11 and TMS 602–11/ACI 530.1–11/ASCE 6–11 (2011) [74] makes no recommendations for the values of the cohesion and friction coefficient to be adopted. Clause 3.3.4 of AS 3700 (2018) [60] also provides a recommendation for the values of cohesion and friction coefficient to be adopted, correlating them with $f_{mt}$.

In the absence of any information on the values of $f_{v0}$ and $\mu$, an empirical formula calculating $\tau_u$ based on $f_{mt}$ values as $\tau_u = 1.6f_{mt} + 0.9\sigma$ developed by Willis [67] is proposed to be used. This proposal is also made because for existing buildings or in an in-situ situation, the bond-wrench test required to evaluate $f_{mt}$ can be carried out with far more ease than the direct shear test on masonry triplets [104] or the shove test [105] required to evaluate $f_{v0}$ and $\mu$ though recommendations for them are usually provided by codes. This empirical formula has also been shown to be conservative by torsional shear tests performed on masonry couplets in [91] for several batches of masonry in clay and CS brick masonry. >85% of all specimens tested in clay and CS brick masonry were measured to exhibit a torsional shear strength higher than that calculated using the proposed formulation. Values of $f_{mt}$ can be adopted as per the recommendations provided in section 4.2. A value of $k_b = 0.208$ was recommended to be used by Willis [67] while using the same formulation.

It is also worthy to note that AS 3700 [60] also provides relationship to estimate the torsional shear strength of masonry bed joints as $\tau_u = 2.25(f_{mt})^{1/2} + 0.15\sigma$. Despite, the relationship being dimensionally inconsistent, considering the variability in response typically associated with masonry in shear and also observed experimentally in [91], such empirical formulation is still useful to provide a reasonable estimate of

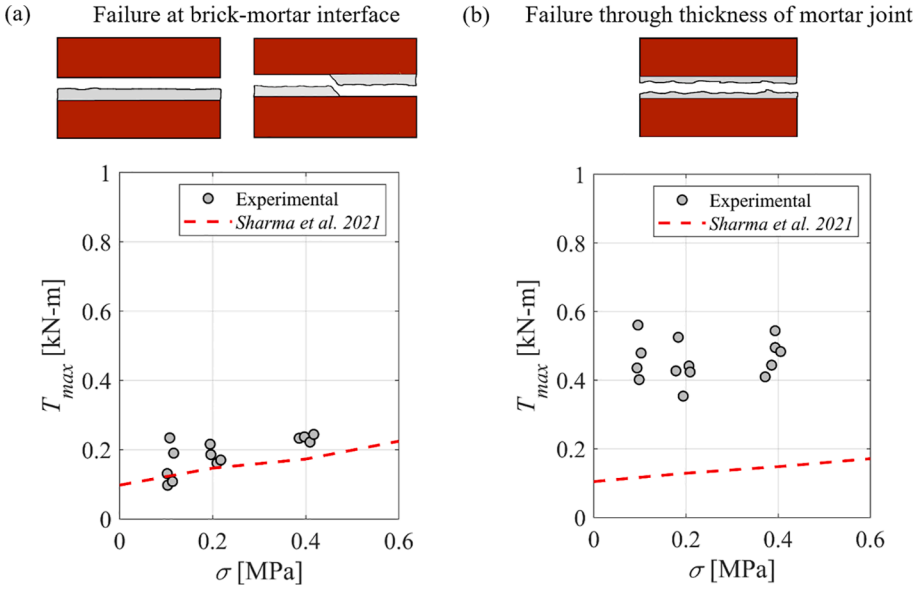


**Fig. 10.** Performance of the torsional shear strength of bed joint ($\tau_u$) formulation by Sharma *et al.* [91] against experimental results of torsional shear tests on masonry couplets when failure under torsional shear (a) is at the brick–mortar interface and (b) is through the thickness of the mortar joint. ($T_{max}$ denotes the peak torque that can be resisted by the bed joint, which can be measured directly experimentally).

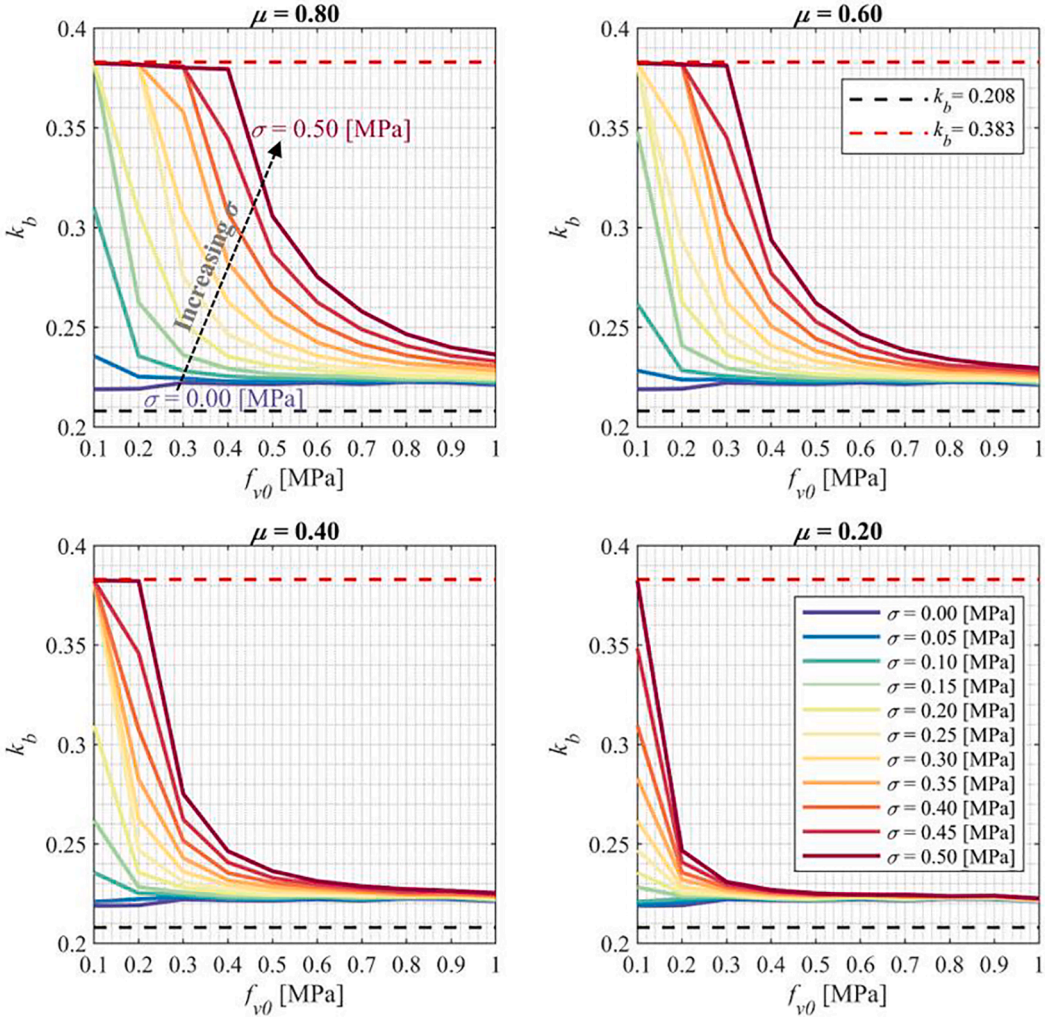


**Fig. 11.** $k_b$ evaluated for combinations of $f_{v0}$ and $\mu$ under the action of different levels of $\sigma$ [91].

the torsional shear strength of bed joint.

## 5. Period of vibration

The period of vibration is a fundamental parameter in force-based methodologies for assessing structures. This parameter defines the spectral acceleration against which the wall should be assessed against *i.e.* the demand in Fig. 1 [107]. To calculate the period corresponding to the fundamental mode of vibration of OOP two-way spanning walls, reference was made to the monograph on the vibration of plates by Leissa [108]. In particular, the solutions for the first mode of vibration of rectangular plates by Janich [109] and Warburton [110]. As per these solutions, the period ($T$) associated with the wall can be calculated as per equation (5):

$$T = \frac{2\pi}{\omega} = \frac{2 \times \pi}{\sqrt{\frac{\pi^4 \times D \times K}{H^4 \times \rho_S \times N}}} = \frac{2 \times H^2}{\pi}\sqrt{\frac{\rho_S \times N}{D \times K}} = \frac{2 \times H^2}{\pi}\sqrt{\frac{\rho_S}{D}} \times C_T \quad (5)$$

where $\omega$ is the angular frequency;

$D$ is the flexural rigidity calculated as $D = \frac{E \times t^3}{12 \times (1-\nu^2)}$ with $t$ referring to the thickness of the wall, $\nu$ to the Poisson's ratio of masonry and $E$ to the modulus of elasticity of the masonry in tension and compression (can be evaluated as per standardized testing procedures in [111,112] and recommendation of values to be adopted are provided are usually provided by codes);

$K$ is a parameter that depends on the aspect ratio ($L/H$) as well as boundary conditions of the wall ([109,110]);

$H$ is the height of the wall;

$\rho_s$ is the mass density per unit area of the wall;

$N$ is a parameter that depends on the boundary conditions of the wall ([109,110]);

To facilitate the use of equation (5), a constant $C_T$ calculated as $C_T = \sqrt{\frac{N}{K}}$ is provided graphically in Fig. 12 for walls of varying aspect ratios in different configurations, assuming $\nu = 0.25$. To be consistent with the methodology for calculating *PCR*, curves corresponding to both $R_f = 0$ and $R_f = 1$ *i.e.* supported vertical edges are simply supported and fully fixed respectively are plotted. Dynamic identification tests had been performed in the reference experimental campaigns [46,47] to evaluate the period associated with the fundamental mode of vibration of all tested specimens. The experimentally measured period of all tested walls other than the specimen fully-fixed on all four sides *i.e.* CS-005-RR in [46], was observed to lie between the $R_f = 0$ and $R_f = 1$ cases (Fig. 12a). The discrepancy in the case of specimen CS-005-RR is presumably because of a mechanical play in the hinges of the experimental setup, not being able to guarantee a complete fixity at the top edge for low amplitude vibrations (*i.e.* the dynamic identification tests) but resulted adequate to represent a fixity in high-amplitude dynamic tests. Another factor could be a horizontal crack near the base of the specimen, that was formed while transporting the specimen onto the shake table (and then restored), before the dynamic identification tests. This was

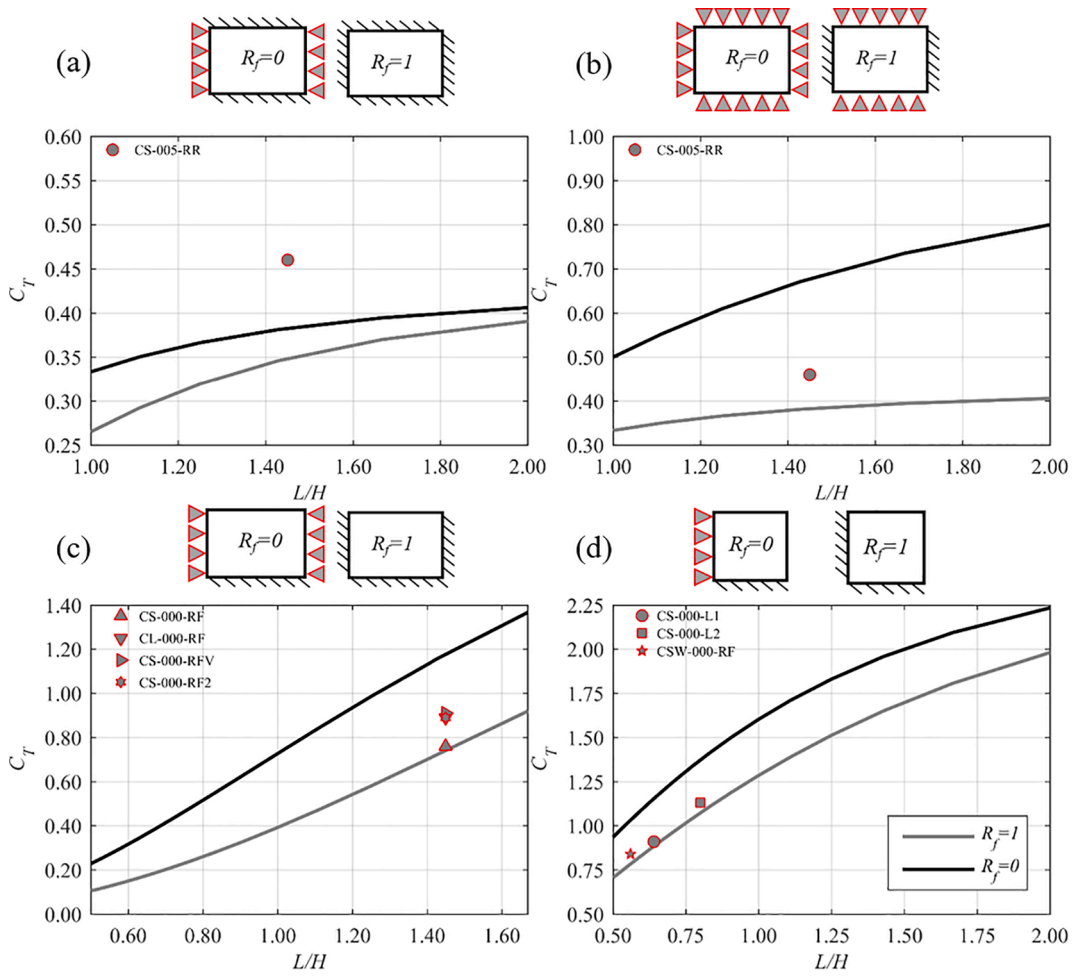


**Fig. 12.** Charts of values of the $C_T$ coefficient for evaluating the fundamental period of vibration of two-way spanning URM walls in different boundary conditions from their aspect ratio ($L/H$): (a-b) walls supported on all four sides; (c) walls supported on three sides but having their top edge free and (d) walls supported on two adjacent sides (note that results corresponding to specimen CS-005-RR are provided in both (a) and (b) to highlight the effect of boundary conditions and damage states on the period of a wall).

verified by considering both the $R_f = 0$ and $R_f = 1$ configurations but with a simple-support condition at the base and top of the wall and the experimentally measured period lies between these limits (Fig. 12b). It is to be noted that these results have not been provided directly in Fig. 12 but in terms of the $C_T$ values required to obtain the experimentally measured period of all specimens. The observation made in case of specimen CS-005-RR highlights the effect that a flexible horizontal diaphragm and/or the damage state could have on the period of vibration of two-way spanning URM walls, which should be inspected carefully to choose the most appropriate configuration from Fig. 12 or others available in [108]. Also for walls with large openings, the special configuration mentioned in section 3.1.2/Fig. 6 can be considered while evaluating their period. The experimentally measured period of the tested specimen with an eccentric opening *i.e.* CSW-000-RF in [46] can be observed to lie within the $R_f = 0$ and $R_f = 1$ limits in Fig. 12d.

The period of vibration is a fundamental parameter in the force-based design of structures as this parameter defines the spectral acceleration and thus the base shear force to which the building should be designed.

## 6. Summary (step-by-step) of the proposed methodology

This section provides a step-by-step summary of how to implement the simplified methodology proposed in this paper:

1. Check if the lateral edges of the wall to be assessed are supported or not. Attention should also be paid to the presence of any existing cracks and construction detailing, especially at all supported edges.
2. The material properties for the URM of the wall being assessed can be evaluated/assumed as per the enlisted testing standards, recommendations from codes or formulation provided in section 4. In particular, Fig. 10 allows to evaluate the factor $k_b$ to estimate the torsional shear strength from the values of $f_{v0}$, $\mu$, and the acting level of vertical compression.
3. If lateral supports are present, the peak cracking resistance (*PCR*) of the two-way spanning wall should be calculated as per the recommendations of section 3. If lateral edges are not supported or pre-cracked, the wall can be treated to be one-way spanning and NLKA methods can be used.
4. For walls with openings and cavity walls, the recommendations provided in section 3.1.1 and 3.1.2 respectively should be referred to. For walls supported on all four edges, in the presence of a slab capable of uplifting the portion of the structure above, the check provided in section 3.1.3 should be carried out. If the check is not satisfactory, the wall should be considered to be free on top.
5. The seismic demand with which the *PCR* has to be compared (*i.e.* floor spectrum) should be calculated corresponding to the period of the wall evaluated as per the recommendations provided in section 4. The presence of any existing cracks should be taken into account

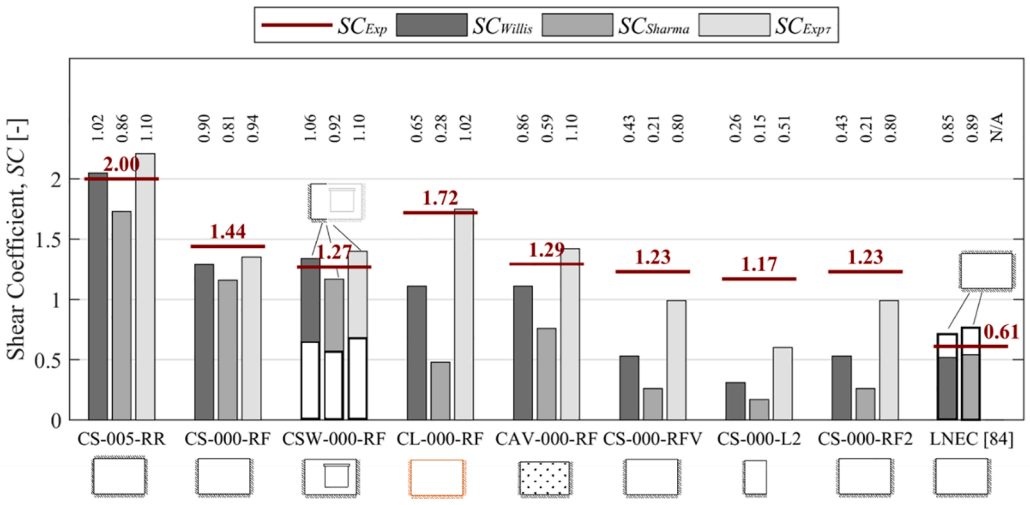


**Fig. 13.** Performance of the proposed simplified methodology against experimental results of walls tested in Graziotti *et al.* [46], Sharma *et al.* [47] and Tomassetti *et al.* [85].

while evaluating the boundary conditions and calculating the period of the wall.

6. If the *PCR* is greater than the evaluated demand, the wall can be considered safe. Otherwise, the post-*PCR* behaviour of the wall should be assessed as per NLKA methods, treating the wall to be one-way spanning. This methodology automatically considers the tendency of long two-way spanning walls with supported vertical edges far apart from each other to behave in OOP one-way bending.

## 7. Performance of the proposed methodology against experimental results

The performance of the proposed methodology is compared with experimental results in this section. The experimental results here correspond to all two-way spanning full-scale URM walls tested dynamically under OOP excitation available in literature *i.e.* walls tested in Graziotti *et al.* [46] (CS-005-RR, CS-000-RF, CL-000-RF, CSW-000-RF and CAV-000-RF in Fig. 13) and Sharma *et al.* [47] (CS-000-RF2, CS-000-L2, CS-000-RFV in Fig. 13). Additionally, the wall of a full-scale building which underwent OOP two-way bending collapse while being tested incrementally dynamically by Tomassetti *et al.* [85] in LNEC, Lisbon was also considered (LNEC in Fig. 13). While more information related to these experimentally tested specimens can be found in [46,47,85], all the details relevant for calculating their *PCR* are summarised in Table 2. The comparison between analytical estimations and experimental measurements of *PCR* for specimens having different masses is provided in terms of a shear coefficient (*SC*) calculated by dividing the inertial force associated with each wall by the weight of its OOP panel. Since complementary material characterization tests evaluating $f_{v0}$ and $\mu$ as well as $f_{mt}$, were performed in all experimental campaigns, the two approaches *i.e.* Sharma *et al.* [91] ($SC_{Sharma}$ in Fig. 13) and Willis [67] ($SC_{Willis}$ in Fig. 13) outlined in section 4.3, to evaluate $\tau_u$ were implemented to analytically evaluate the *PCR* associated with the experimentally tested walls. This is also because the bond-wrench test to evaluate $f_{mt}$ used to calculate $\tau_u$ in the Willis [67] relationship can be carried out more easily in an *in-situ* condition than the direct shear tests on masonry triplets or the shove test required to evaluate $f_{v0}$ and $\mu$. An additional analytical calculation of *SC* is also done, adopting directly the experimentally measured torsional shear results ($SC_{Exp\tau}$ in Fig. 13). This is because failure for masonry couplets tested under torsional shear corresponding to both experimental campaigns [46,47] occurred through the thickness of the mortar joint (see Fig. 10b). As already highlighted in section 4.3, for such batches of masonry the $\tau_u$ formula developed by Sharma *et al.* [91] underestimates the torsional shear strength of bed joints. Such an experimental evaluation of $\tau_u$ was not performed in [85], and consequently this direct approach could not be implemented. All analytical calculations reported were performed adopting the recommended $R_f$ value of 0.5. The ratio of $SC_{Exp}$ to *SC* values calculated analytically is also provided on top of each bar of the histogram in Fig. 13.

It can be easily gleaned from Fig. 13, that $SC_{Sharma}$ values are always safely conservative with respect to what was measured experimentally, $SC_{Exp}$. The significant underestimation of $SC_{Sharma}$ in case of some specimens (especially CL-000-RF, CS-000-RFV, CS-000-RF2) can be attributed to the already mentioned observation that the Sharma *et al.* [91] $\tau_u$ formulation under predicts the torsional shear strength of bed joints when the failure surface under torsional shear passes through the thickness of the mortar joint. This has been highlighted in section 8 as an open issue of the proposed methodology warranting further research and for more details on this, a reader is referred to [91]. Such underestimations, gets corrected when the experimentally measured torsional shear results are directly used *i.e.* $SC_{Exp\tau}$ in Fig. 13. Comparisions of $SC_{Willis}$ with $SC_{Exp}$ are largely favourable, withstanding the slight overestimation in the case of specimen CS-005-RR. Understimations of $SC_{Exp}$ using the $SC_{Willis}$ approach also (similar to $SC_{Sharma}$) can be observed for specimens CS-000-RFVand CS-000-RF2. All analytical methods underestimate $SC_{Exp}$ in case of CS-000-L2, a specimen free on adjacent vertical and horizontal edges. This has also been highlighted as an open issue of the proposed methodology in section 8.

Regarding the special considerations outlined in section 3.1: in the case of specimen CSW-000-RF [46], a specimen with an opening occupying 25% of its area, considering the special configuration recommended in section 3.1.1, leads to a significant improvement of the analytical estimations (bars in grey correspond to the recommended special configuration *i.e.* free at window edges, bars in white to normal configuration) with respect to the experimentally measured value. Similarly, for CAV-000-RF, a cavity wall composed of leaves in CS and clay brick masonry *i.e.* CAV-000-RF (CS) and CAV-000-RF (CL) respectively in Table 2, connected by ties at a density of 2 ties/m$^2$, analytical estimations of *SC* calculated taking the sum of the *PCR* of the individual leaves gave a very reasonable estimation of the $SC_{Exp}$ of the cavity wall. Also, the importance of the check provided in section 3.1.3 is highlighted by the application of the proposed methodology for a wall which underwent an OOP two-way bending collapse in a full-scale building *i.e.* LNEC[85] in Table 2/Fig. 13. When considering this wall to be restrained on all four sides, an unconservative overestimation of $SC_{Exp}$ is made. This is corrected when adopting the proposed check, accounting for the inability of the slab on top of the wall to accommodate the uplift

**Table 2**
Details used to apply the proposed simplified methodology for dynamically tested two-way spanning full-scale URM walls [46,47,85].

| | | | | | | | | | | | | | Sharma *et al.* [89] $\tau_u = f_{v0} + \mu\sigma$ | | | | Willis [67] $\tau_u = 1.6f_{mt} + 0.9\sigma$ | | | Experimental $\tau_u$ $\tau_u$ *measured* | | | |
|---|---|---|---|---|---|---|---|---|---|---|---|---|---|---|---|---|---|---|---|---|---|---|---|
| ***Specimen*** | ***Description*** | ***Mass*** [kg] | ***HE*** [#] | ***VE*** [#] | ***Op*** [-] | $L_d$ [m] | $H_d$ [m] | $\alpha$ [-] | $a_f$ [-] | $k_1$ [-] | $k_2$ [-] | $f_{v0}$ [MPa] | $\mu$ [-] | $k_b$ [-] | $SC_{Sharma}$ [-] | $f_{mt}$ [MPa] | $k_b$ [-] | $SC_{Willis}$ [-] | $\tau_u$ [MPa] | $k_b$ [-] | $SC_{Expτ}$ [-] | $SC_{Exp}$ [-] |
| **CS-005-RF** | **Single leaf CS brick masonry wall subjected to a pre-compression of 0.05 MPa** | 2056 | 2 | 2 | n | 2.0 | 1.4 | 1.1 | 1.5 | 0.5 | 2.9 | 0.81 | 0.46 | 0.222 | 1.73 | 0.95 | 0.208 | 2.05 | 1.84 | 0.208 | 2.21 | 2.00 |
| **CS-000-RF** | **Single leaf CS brick masonry wall** | 2056 | 1 | 2 | n | 2.0 | 2.8 | 0.5 | 1.2 | 1 | 1.5 | 0.81 | 0.46 | 0.222 | 1.16 | 0.95 | 0.208 | 1.29 | 1.84 | 0.208 | 1.35 | 1.44 |
| **CSW-000-RF** | **Single leaf CS brick masonry wall with eccentric opening** | 1530 | 1 | 1 | n | 1.5 | 2.8 | 0.4 | 1.2 | 0.5 | 1.2 | 0.81 | 0.46 | 0.222 | 1.17 [0.56]* | 0.95 | 0.208 | 1.34 [0.64]* | 1.84 | 0.208 | 1.40 [0.67]* | 1.27 |
| **CL-000-RF** | **Single leaf clay brick masonry wall** | 2178 | 1 | 2 | n | 2.0 | 2.8 | 0.4 | 1.2 | 1.1 | 1.7 | 0.18 | 0.63 | 0.222 | 0.48 | 0.41 | 0.208 | 1.11 | 1.08 | 0.208 | 1.75 | 1.72 |
| **CAV-000-RF (CS)** | **CS brick masonry leaf of a cavity wall (tie density = 2 ties/m$^2$)** | 2056 | 1 | 2 | n | 2.0 | 2.8 | 0.5 | 1.2 | 1 | 1.5 | 0.81 | 0.46 | 0.222 | 0.76 | 0.95 | 0.208 | 1.11 | 1.84 | 0.208 | 1.42 | 1.29 |
| **CAV-000-RF (CL)** | **Clay brick masonry leaf of a cavity wall (tie density = 2 ties/m2)** | 2375 | 1 | 2 | n | 2.2 | 2.7 | 0.4 | 1.2 | 1.1 | 1.9 | 0.18 | 0.63 | 0.222 | | 0.41 | 0.208 | | 1.08 | 0.208 | | |
| **CS-000-RFV** | **Single leaf CS brick masonry wall** | 2056 | 1 | 2 | n | 2.0 | 2.8 | 0.5 | 1.2 | 1 | 1.5 | 0.13 | 0.55 | 0.219 | 0.26 | 0.22 | 0.208 | 0.53 | 1.39 | 0.208 | 0.99 | 1.23 |
| **CS-000-L2** | **Single leaf CS brick masonry wall** | 1140 | 1 | 1 | n | 2.2 | 2.8 | 1.2 | 0.5 | 1.1 | 6.6 | 0.13 | 0.55 | 0.219 | 0.17 | 0.22 | 0.208 | 0.31 | 1.39 | 0.208 | 0.60 | 1.17 |
| **CS-000-RF2** | **Single leaf CS brick masonry wall** | 2056 | 1 | 2 | n | 2 | 2.8 | 0.5 | 1.2 | 1 | 1.5 | 0.13 | 0.55 | 0.219 | 0.26 | 0.22 | 0.208 | 0.53 | 1.39 | 0.208 | 0.99 | 1.23 |
| **LNEC** | **Single leaf CS brick masonry wall in a building** | 2439 | 1 | 2 | n | 2.5 | 2.4 | 0.8 | 1.3 | 0.7 | 2.2 | 0.45 | 0.48 | 0.222 | 0.54 [0.75]* | 0.36 | 0.208 | 0.52 [0.72]* | N/A | N/A | N/A | 0.61 |

***HE*** and ***VE*** indicate the number of restrained horizontal and vertical edges respectively - ***Op*** indicates presence (y) or absence (n) of an opening in the analytical idealization - * indicates values obtained not considering section 3.1.1 and 3.1.3.

induced by the adjacent in-plane piers and subsequently considering the wall to be free on top (bars in grey correspond to the recommended special configuration: free on top, bars in white correspond to normal configuration: fixed on all four sides).

Dynamic identification tests were also performed on walls tested in both Graziotti *et al.* [46] and Sharma *et al.* [47], to experimentally measure the period associated with their fundamental natural mode of vibration. It has already been demonstrated in Fig. 12 on how the theory of vibration of plates, proposed to be used in the methodology for the calculating the period of two-way spanning URM walls could estimate well the experimentally measured values. Estimation of the period is fundamental to evaluate the acceleration demand on the wall being assessed. The period of such elements lies between 0 and 0.1 s, a range in which the aceeleration demand may vary significantly (even 2 to 3 times higher from PGA to the plateau spectral acceleration). This makes an accurate estimation of the period of these structural components very important.

If the *PCR* is lower than the spectral acceleration demand, NLKA methods which do not consider the presence of lateral supports (*i.e.* assume a one-way bending configuration) are proposed to be safely used. This recommendation is based on the one-way bending behaviour exhibited by a majority of Weak Unit-Strong Joint URM walls *i.e.* walls constructed in masonry exhibiting line failure under pure horizontal bending, in both reference experimental studies [46,47] immediately after the attainment of their *PCR* (Fig. 2).

## 8. Open issues

This section highlights several issues which have not been adequately understood and present interesting avenues for further development of the simplified methodology proposed in this paper:

- The factor $R_f$ controlling (see Table 1) the value of $k_1$ in equation (1) has been formulated currently only to account for the degree of rotational restraint at supported vertical edges. However, this factor also implicitly controls the contribution of $M_h$ *i.e.* horizontal bending (see equation (2)) at the instant, the peak cracking resistance of the wall *i.e. PCR* is attained. It has also been remarked in [47], that a value of $R_f = 0.5$ (as recommended to be adopted) could give a good fit with experimental results [46,47,39,77] as a result of peak crack capacities not being attained all at the same instant, rather than a boundary condition intermediate between simple-support ($R_f = 0$) and fully-fixed ($R_f = 1$) being realised. Further work is required, to formulate values of $R_f$ accounting for the effects of boundary conditions at the supported edges as well as weighted contributions to *PCR* from $M_h$. Such studies should also similarly address the contribution of diagonal bending *i.e.* $M_d$ to *PCR*.
- A common observation from the incremental dynamic testing of Weak Unit-Strong Joint walls, exhibiting line failure under horizontal bending, in both reference experimental campaigns [46,47] was the non-occurrence of diagonal cracks in certain configurations (see Fig. 2). Explicit application of the virtual work method to the experimentally observed failure mechanisms (as reported in [46]) also seems to indicate that diagonal cracks might not have any or a non-significant contribution to the peak strength of such walls in certain boundary conditions. The virtual work method also underestimated the experimental *PCR* associated with a wall having adjacent vertical and horizontal edges unrestrained. Such issues need to be explored and if required the abacus of failure mechanisms (Fig. 3) considered by the methodology needs to be expanded.
- Improvements have been made in the approach adopted to calculate the torsional shear strength of bed joints, departing from empirical formulation to more mechanically sound approaches. Nevertheless, significantly higher torsional shear strength than what is calculated using the formula proposed by Sharma *et al.* [91], adopting direct shear parameters *i.e.* cohesion and friction coefficient was exhibited experimentally by masonry couplets in which failure under torsional shear was through the thickness of the mortar joint. For the same batches, failures in direct shear tests which were used to obtain input parameters of the proposed formulation were limited to the unit-mortar interface. Further research is warranted to better understand this observation. Sharma *et al.* [91] also observed through experiments and co-ordinated numerical modelling exercises, possible effects of dilatancy on the torsional shear strength of masonry couplets while developing the formulation highlighted in section 4.3. The effect of the dilatancy (if any) on the OOP strength of two-way spanning URM walls needs to be studied further.
- The effect of having different excitations at the top and base, as studied for one-way URM walls by Tondelli *et al.* [113] on the response of two-way spanning URM walls should be assessed both experimentally and numerically.
- Weak Unit- Strong Joint and Strong Unit-Weak Joint URM walls, exhibiting line and stepped failure under horizontal bending respectively were observed to exhibit significantly different post-*PCR* behaviour in the reference experimental campaigns [46,47]. The OOP collapse vulnerability of two-way spanning URM walls in these two different typologies of URM should be studied and compared.

## 9. Concluding remarks

A number of guidelines for masonry structures currently do not appropriately account for the OOP two-way bending behaviour of URM walls. Some guidelines do not account for the presence of lateral supports: considering two-way bending as one-way bending. This assumption has been evidenced by recent incremental dynamic experiments on full-scale two-way spanning URM walls to be overly conservative. Other guidelines which account for the presence of lateral supports, have conceptual flaws associated with how they account for two-way bending behaviour. This paper attempts to overcome such shortcomings by proposing a methodology that can be seamlessly integrated into the existing frameworks of most guidelines for masonry structures.

The methodology involves a check based on the virtual work method, to account for the significant cracking resistance exhibited by two-way spanning URM walls. Additional checks were developed based on experimental observations for walls with large openings, cavity walls and change in boundary conditions of OOP walls in the presence of stiff floor systems during seismic loading. The formulation to calculate the peak cracking resistance, necessary for carrying out the proposed check, has also been improved in terms of the approach for calculating the torsional shear strength of masonry bed joints. As per the new approach, the torsional shear strength can now be calculated from the cohesion and friction coefficient, which can be estimated from standardised testing procedures or recommendations for which are provided in most guidelines addressing masonry structures, departing from previous empirical approaches. Testing standards that can be used to experimentally evaluate the required input material parameters to calculate the peak cracking resistance or recommendations in building codes addressing the same are enlisted and reviewed. Charts based on plate theory are then provided to calculate the period associated with the fundamental mode of vibration of two-way spanning URM walls. The period is of fundamental importance when computing the seismic demand, against which the peak cracking resistance has to be checked. Ultimately, open issues which have still not been adequately understood and require further research effort are highlighted. In this context, it is to be noted that all data corresponding to the experimental studies adopted as a reference in this study is freely available from the associated data papers [84,114] or can be requested online from www.eucentre.it/nam-project.

## Declaration of Competing Interest

The authors declare that they have no known competing financial

interests or personal relationships that could have appeared to influence the work reported in this paper.

## Acknowledgements

This article reports studies performed as a part of the "Study of the vulnerability of masonry buildings in Groningen" project at the EUCENTRE, undertaken within the framework of the research program for investigating the hazard and risk of induced seismicity in Groningen sponsored by the Nederlandse Aardolie Maatschappij BV. The valuable advice of A. Penna, R. Pinho, M.C. Griffith and J. Vaculik is gratefully acknowledged. Special thanks to J. Uilenreef and L. Grottoli for the practical support. The authors would like to thank all the technical staff at EUCENTRE and University of Pavia (DICAr) laboratories that performed the tests.

## References

[1] Paulay T, Priestly MJN. Seismic Design of Reinforced Concrete and Masonry Buildings. Hoboken, NJ, USA: John Wiley & Sons, Inc.; 1992. 10.1002/9780470172841.
[2] Menon A, Magenes G. Definition of Seismic Input for Out-of-Plane Response of Masonry Walls: I. Parametric Study. J Earthq Eng 2011;15:165–94. https://doi.org/10.1080/13632460903456981.
[3] Drysdale RG, Hamid AA, Baker L. Masonry structures: behavior and design. Englewood Cliffs, New Jersey: Prentice-Hall; 1994.
[4] Krauss EE, Vogdes J. Preliminary outline of program of research in reinforced masonry. J Am Ceram Soc 1932;15:305. https://doi.org/10.1111/j.1151-2916.1932.tb13935.x.
[5] Granholm H. Armerade tegelkonstruktioner.(Reinforced brick structures). Gothenburg, Sweden: 1943.
[6] Losberg A, Johansson S. Sideways Pressure on Masonry Walls of Brickwork. CIB Symp. Bear Walls, Warsaw, Poland. 1969.
[7] Satti KMH. Model brickwork panels under lateral loading. University of Edinburgh 1972.
[8] Satti KMH, Hendry A. The modulus of rupture of brickwork. Essen, Germany: Third Int. Brick Mason. Conf; 1973.
[9] Kheir AMA. Brickwork Panels under Lateral Loading. University of Edinburgh 1975.
[10] Hallquist A. Lateral Loads on Masonry Walls. Oslo, Norway: 1970.
[11] Anderson C. Lateral loading tests on concrete block walls. Struct Eng 1976.
[12] West HWH, Hodgkinson HR. The resistance of brickwork to lateral loading, Part I: Experimental methods and results of tests on small specimens and full sized walls. Struct Eng 1977;10.
[13] Haseltine BA, Tutt JN, West HWH. The resistance of brickwork to lateral loading. Part II: Design of walls to resist lateral loads. Struct Eng 1977:10.
[14] West HWH, Hodgkinson HR, de Vekey R. The lateral resistance of cavity wall with different type of wall ties. Proc. 5th Int. Brick Mason. Conf., Washington, DC, United States: 1979, p. 387–90.
[15] West HWH, Hodgkinson HR, Haseltine BA. The lateral resistance of wall with one free vertical edge. Proc. 5th Int. Brick Mason. Conf., Washington, DC, United States: 1979, p. 382–6.
[16] de Vekey R, Bright N, Luckin K, Arora S. The resistance of masonry to lateral loading, Part III: Research results on autoclaved aerated concrete blockwork. Struct Eng 1986;64A:332–40.
[17] Haseltine BA, Tutt JN. The resistance of brickwork to lateral loading Part IV: Implications of research on design reccomendations. Struct Eng 1986;11:341–50.
[18] Lawrence SJ. Behaviour of brick masonry walls under lateral loading. The University of New South Wales; 1983.
[19] Anderson C. Tests on walls subjected to uniform lateral loading and edge loading. Proc. 7th Int. Brick Mason. Conf., Melbourne, Australia: 1985.
[20] Gairns D., Scrivener J. The flexural strength of concrete block and clay brick masonry panels. Proc. 1st Natl. Struct. Eng. Conf., Melbourne, Australia: 1983.
[21] Southcombe C, Tapp A. An investigation of laterally loaded brickwork panels with openings. Mason Int 1988;2:112–4.
[22] Candy CC., Carrick JW, Shackel B. An evaluation of the energy line method for predicting ultimate load capacity from tests of minimally supported walls subjected to lateral loading. 1989.
[23] Chong VL. The behaviour of laterally loaded masonry panels with openings. University of Pymouth 1993.
[24] Abrams DP, Angel R, Uzarski J. Out-of-plane strength of unreinforced masonry infill panels. Earthq Spectra 1996. https://doi.org/10.1193/1.1585912.
[25] Hendry AW, Hendry AW. Laterally loaded unreinforced walls. Struct. Brickwork 1981. https://doi.org/10.1007/978-1-349-81439-8_5.
[26] Calvi GM, Kingsley GR, Magenes G. Testing of masonry structures for seismic assessment. Earthq Spectra 1996;12:145–62. https://doi.org/10.1193/1.1585872.
[27] Graziotti F, Penna A, Magenes G. A comprehensive in situ and laboratory testing programme supporting seismic risk analysis of URM buildings subjected to induced earthquakes. Bull Earthq Eng 2018. https://doi.org/10.1007/s10518-018-0478-6.
[28] Magenes G, Calvi GM. In-plane seismic response of brick masonry walls. Earthq Eng Struct Dyn 1997;26:1091–112. https://doi.org/10.1002/(SICI)1096-9845(199711)26:11<1091::AID-EQE693>3.0.CO;2-6.
[29] Tomaževič M, Klemenc I. Seismic behaviour of confined masonry walls. Earthq Eng Struct Dyn 1997;26:1059–71. https://doi.org/10.1002/(SICI)1096-9845(199710)26:10<1059::AID-EQE694>3.0.CO;2-M.
[30] Anthoine A, Magonette G, Magenes G. Shear-compression testing and analysis of brick masonry walls. Proc. 10th Eur. Conf. Earthq. Eng., Vienna, Austria: 1995.
[31] Paquette J, Bruneau M. Pseudo-dynamic testing of unreinforced masonry building with flexible diaphragm. J Struct Eng 2003;129:708–16. https://doi.org/10.1061/(ASCE)0733-9445(2003)129:6(708).
[32] Griffith MC, Lam NTK, Wilson JL, Doherty K. Experimental investigation of unreinforced brick masonry walls in flexure. J Struct Eng 2004;130:423–32. https://doi.org/10.1061/(ASCE)0733-9445(2004)130:3(423).
[33] Simsir CC, Aschheim MA, Abrams DP. Out-of-plane dynamic response of unreinforced bearing walls attached to flexible diaphragms. Proc. 13th World Conf. Earthq. Eng., Vancouver, British Columbia, Canada: 2004.
[34] Penner O, Elwood KJ. Out-of-plane dynamic stability of unreinforced masonry walls in one-way bending: Shake table testing. Earthq Spectra 2016. https://doi.org/10.1193/011415EQS009M.
[35] Giaretton M, Dizhur D, Ingham JM. Dynamic testing of as-built clay brick unreinforced masonry parapets. Eng Struct 2016;127:676–85. https://doi.org/10.1016/j.engstruct.2016.09.016.
[36] Graziotti F, Tomassetti U, Penna A, Magenes G. Out-of-plane shaking table tests on URM single leaf and cavity walls. Eng Struct 2016;125. https://doi.org/10.1016/j.engstruct.2016.07.011.
[37] Restrepo-Vélez LF, Magenes G, Griffith MC. Dry stone masonry walls in bending - Part I: Static tests. Int J Archit Herit 2014;8:1–28. https://doi.org/10.1080/15583058.2012.663059.
[38] Vaculik J, Griffith MC, Hogarth B, Todd J. Out-of-plane flexural response tests using dry-stack masonry. Proc. Aust. Earthq. Soc. Conf Mt Gambier, South Australia. 2004.
[39] Griffith MC, Vaculik J, Lam NTK, Wilson J, Lumantarna E. Cyclic testing of unreinforced masonry walls in two-way bending. Earthq Eng Struct Dyn 2007;36:801–21. https://doi.org/10.1002/eqe.654.
[40] Vaculik J, Griffith MC. Out-of-plane shaketable testing of unreinforced masonry walls in two-way bending. Bull Earthq Eng 2018. https://doi.org/10.1007/s10518-017-0282-8.
[41] Messali F, Ravenshorst G, Esposito R, Rots JG. Large-scale testing program for the seismic characterization of Dutch masonry walls. 16th World Conf Earthq 2017: Paper N° 4753.
[42] Damiola M, Esposito R, Messali F, Rots JG. Quasi-static cyclic two-way out-of-plane bending tests and analytical models comparison for URM walls. Proc. 10th Int. Mason. Conf., Milan, Italy: 2018.
[43] Maccarini H, Vasconcelos G, Rodrigues H, Ortega J, Lourenço PB. Out-of-plane behavior of stone masonry walls: Experimental and numerical analysis. Constr Build Mater 2018;179:430–52. https://doi.org/10.1016/j.conbuildmat.2018.05.216.
[44] Walsh KQ, Dizhur D, Shafaei J, Derakhshan H, Ingham JM. In Situ Out-of-Plane Testing of Unreinforced Masonry Cavity Walls in as-Built and Improved Conditions. Structures 2015;3:187–99. https://doi.org/10.1016/j.istruc.2015.04.005.
[45] Padalu PKVR, Singh Y, Das S. Cyclic two-way out-of-plane testing of unreinforced masonry walls retrofitted using composite materials. Constr Build Mater 2020;238:117784. https://doi.org/10.1016/j.conbuildmat.2019.117784.
[46] Graziotti F, Tomassetti U, Sharma S, Grottoli L, Magenes G. Experimental response of URM single leaf and cavity walls in out-of-plane two-way bending generated by seismic excitation. Constr Build Mater 2019;195:650–70. https://doi.org/10.1016/j.conbuildmat.2018.10.076.
[47] Sharma S, Tomassetti U, Grottoli L, Graziotti F. Two-way bending experimental response of URM walls subjected to combined horizontal and vertical seismic excitation. Eng Struct 2020;219:110537. https://doi.org/10.1016/j.engstruct.2020.110537.
[48] Petracca M, Pelà L, Rossi R, Oller S, Camata G, Spacone E. Multiscale computational first order homogenization of thick shells for the analysis of out-of-plane loaded masonry walls. Comput Methods Appl Mech Eng 2017;315:273–301. https://doi.org/10.1016/j.cma.2016.10.046.
[49] Tomassetti U, Graziotti F, Penna A, Magenes G. Modelling one-way out-of-plane response of single-leaf and cavity walls. Eng Struct 2018. https://doi.org/10.1016/j.engstruct.2018.04.007.
[50] D'Altri AM, de Miranda S, Castellazzi G, Sarhosis V. A 3D detailed micro-model for the in-plane and out-of-plane numerical analysis of masonry panels. Comput Struct 2018;206:18–30. https://doi.org/10.1016/j.compstruc.2018.06.007.
[51] Godio M, Beyer K. Trilinear model for the out-of-plane seismic assessment of vertically spanning unreinforced masonry walls. J Struct Eng 2019;145:04019159. https://doi.org/10.1061/(ASCE)ST.1943-541X.0002443.
[52] AlShawa O, Sorrentino L, Liberatore D. Simulation Of shake table tests on out-of-plane masonry buildings. Part (II): combined finite-discrete elements. Int J Archit Herit 2016;1–15. https://doi.org/10.1080/15583058.2016.1237588.
[53] Silva LC, Lourenço PB, Milani G. Nonlinear discrete homogenized model for out-of-plane loaded masonry walls. J Struct Eng 2017. https://doi.org/10.1061/(asce)st.1943-541x.0001831.
[54] Malomo D, Morandini C, Crowley H, Pinho R, Penna A. Impact of ground floor openings percentage on the dynamic response of typical Dutch URM cavity wall structures. Bull Earthq Eng 2021;19:403–28. https://doi.org/10.1007/s10518-020-00976-z.

[55] Silva LC, Lourenço PB, Milani G. Numerical homogenization-based seismic assessment of an English-bond masonry prototype: structural level application. Earthq Eng Struct Dyn 2020. https://doi.org/10.1002/eqe.3267.
[56] Vanin F, Penna A, Beyer K. Equivalent-frame modeling of two shaking table tests of masonry buildings accounting for their out-of-plane response. Front Built Environ 2020;6. https://doi.org/10.3389/fbuil.2020.00042.
[57] Lourenço PB. Computations on historic masonry structures. Prog Struct Eng Mater 2002. https://doi.org/10.1002/pse.120.
[58] Kappos AJ, Penelis GG, Drakopoulos CG. Evaluation of Simplified Models for Lateral Load Analysis of Unreinforced Masonry Buildings. J Struct Eng 2002;128:890–7. https://doi.org/10.1061/(ASCE)0733-9445(2002)128:7(890).
[59] EN 1996-1-1: Eurocode 6: Design of masonry structures - Part 1: General rules for reinforced and unreinforced masonry structures. Brussels, Belgium: European Standards, CEN/TC; 2006.
[60] AS 3700-2018:Masonry Structures, Australian Standard, Sydney, Australia 2018.
[61] CSA Standard (2004): CSA S304-14 – Design of masonry structures. Ontario, Canada. Canadian Standards Association, CSA; n.d.
[62] Johansen K. Yield-Line Theory. London: Cement and Concrete Association; 1962.
[63] Drysdale RG, Baker C. Failure Line design of unreinforced masonry walls subjected to out-of-plane loading. Hamilton. Ontario, Canada: 2003.
[64] Sinha BP. Simplified Ultimate Load Analysis of Laterally Loaded Model Orthotropic Brickwork Panels of Low Tensile Strength. Struct Eng Eng 1978;56B:81–4.
[65] Sinha B. An ultimate load analysis of laterally loaded brickwork panels. Int J Mason Constr 1980;1:57–61.
[66] Lawrence S, Marshall R. Virtual work design method for masonry panels under lateral load. In: 12th Int Brick/Block Mason Conf; 2000. p. 1063–73.
[67] Willis C. Design of unreinforced masonry walls for out-of-plane loading. University of Adelaide; 2004.
[68] Willis CR, Griffith MC, Lawrence SJ. Moment capacities of unreinforced masonry sections in bending. Aust J Struct Eng 2006;6:133–46. https://doi.org/10.1080/13287982.2006.11464950.
[69] Griffith MC, Lawrence SJ, Willis C. Diagonal Bending of Unreinforced Clay Brick Masonry. Mason Int 2005;18:125–38.
[70] Vaculik J. Unreinforced masonry walls subjected to out-of-plane seismic actions. University of Adelaide; 2012.
[71] Maluf D., Parsekian G., Shrive N. An investigation of the out-of-plane loaded unreinforced masonry walls design criteria. Proc. 14th Int. Brick Block Mason. Conf., Sydney, Australia: 2008.
[72] Chang L-Z, Messali F, Esposito R. Capacity of unreinforced masonry walls in out-of-plane two-way bending: A review of analytical formulations. Structures 2020;28:2431–47. 10.1016/j.istruc.2020.10.060.
[73] NZSEE. Section C8 – Seismic assessment of unreinforced masonry buildings, The seismic assessment of existing buildings: Technical guidelines for engineering assessment 2016.
[74] TMS 402-11/ ACI 530-11/ ASCE 5-11 & TMS 602-11/ ACI 530.1-11/ ASCE 6-11. Building Code Requirements and Specification for Masonry Structures Masonry Standard Joint Committee (MSJC); 2011.
[75] EN 1052-5. Methods of test for masonry – Part 5: Determination of bond strength by the bond wrench method. Brussels, Belgium: European Standards, CEN/TC; 2005.
[76] LUM B2 Bond strength of masonry using the bond wrench method. RILEM Recomm. Test. Use Constr. Mater., E & FN SPON; 1994, p. 481–3.
[77] Vaculik J, Griffith MC. Out-of-plane shaketable testing of unreinforced masonry walls in two-way bending. Springer Netherlands; 2017. 10.1007/s10518-017-0282-8.
[78] Derakhshan H, Griffith MC, Ingham JM. Out-of-Plane Behavior of One-Way Spanning Unreinforced Masonry Walls. J Eng Mech 2013;139:409–17. https://doi.org/10.1061/(ASCE)EM.1943-7889.0000347.
[79] Derakhshan H, Dizhur D, Griffith MC, Ingham JM. Seismic Assessment of Out-of-Plane Loaded Unreinforced Masonry Walls. Bull New Zeal Soc Earthq Eng 2014;47:119–38.
[80] Vaculik J, Griffith MC. Probabilistic analysis of unreinforced brick masonry walls subjected to horizontal bending. J Eng Mech 2017;143. https://doi.org/10.1061/(ASCE)EM.1943-7889.0001266.
[81] Vaculik J, Griffith MC. Out-of-plane load–displacement model for two-way spanning masonry walls. Eng Struct 2017;141:328–43. https://doi.org/10.1016/j.engstruct.2017.03.024.
[82] Padalu PKVR, Singh Y, Das S. Analytical modelling of out-of-plane flexural response of unreinforced and strengthened masonry walls. Eng Struct 2020;218:110797. https://doi.org/10.1016/j.engstruct.2020.110797.
[83] Magenes G, Modena C, da Porto F, Morandi P. Seismic behaviour and design of new masonry buildings: recent developments and consequent effects on design codes. Eurocode 8 Perspect. from Ital. Standpoint Work., 2009.
[84] Tomassetti U, Grottoli L, Sharma S, Graziotti F. Dataset from dynamic shake-table testing of five full-scale single leaf and cavity URM walls subjected to out-of-plane two-way bending. Data Br 2019. https://doi.org/10.1016/j.dib.2019.103854.
[85] Tomassetti U, Correia AA, Candeias PX, Graziotti F, Campos Costa A. Two-way bending out-of-plane collapse of a full-scale URM building tested on a shake table. Bull Earthq Eng 2019;17:2165–98. https://doi.org/10.1007/s10518-018-0507-5.
[86] Beyer K, Tondelli M, Petry S, Peloso S. Dynamic testing of a four-storey building with reinforced concrete and unreinforced masonry walls: prediction, test results and data set. Bull Earthq Eng 2015;13:3015–64. https://doi.org/10.1007/s10518-015-9752-z.
[87] Senaldi I, Magenes G, Penna A, Galasco A, Rota M. The Effect of Stiffened Floor and Roof Diaphragms on the Experimental Seismic Response of a Full-Scale Unreinforced Stone Masonry Building. J Earthq Eng 2014;18:407–43. https://doi.org/10.1080/13632469.2013.876946.
[88] Miglietta M, Damiani N, Guerrini G, Graziotti F. Full-scale shake-table tests on two unreinforced masonry cavity-wall buildings: effect of an innovative timber retrofit. Bull Earthq Eng 2021. https://doi.org/10.1007/s10518-021-01057-5.
[89] Messali F, Rots JG. In-plane drift capacity at near collapse of rocking unreinforced calcium silicate and clay masonry piers. Eng Struct 2018;164:183–94. https://doi.org/10.1016/j.engstruct.2018.02.050.
[90] NPR 9998. Beoordeling van de constructieve veiligheid van een gebouw bij nieuwbouw, verbouw en afkeuren - Geïnduceerde aardbevingen -Grondslagen, belastingen en weerstanden. Delft, The Netherlands: Dutch Practical Guideline, NEN; 2018.
[91] Sharma S, Graziotti F, Magenes G. Torsional Shear Strength of Unreinforced Brick Masonry Bed Joints. Constr Build Mater 2021;275. https://doi.org/10.1016/j.conbuildmat.2020.122053.
[92] RILEM TC. LUM A2 Flexural strength of masonry units, 1991. RILEM Recomm. Test. Use Constr. Mater., E & FN SPON; 1994, p. 459–61.
[93] ASTM C1006-07. Standard Test Method for Splitting Tensile Strength of Masonry Units, West Conshohocken, PA, USA: ASTM Standard, ASTM International; 2007.
[94] AS/NZS 4456.15-2003:Masonry units and segmental pavers and flags - Methods of test - Determining lateral modulus of rupture, Australian Standard, Sydney, Australia n.d.
[95] EN 1998-1-1: Eurocode 8: Design of structures for earthquake resistance. Brussels, Belgium: European Standards, CEN/TC; 1998.
[96] EN 772-1. Methods of test for masonry units – Part 1: Determination of compressive strength. European Standards, CEN/TC, Brussels, Belgium; 2011.
[97] LUM A1 Compressive strength of masonry units. RILEM Recomm. Test. Use Constr. Mater., E & FN SPON; 1994, p. 456–8.
[98] ASTM C140/C140M-20. Standard test methods for sampling and testing concrete masonry units and related units. West Conshohocken, PA, USA: ASTM Standard, ASTM International; 2020.
[99] AS/NZS 4456.4-2003:Masonry units and segmental pavers and flags - Methods of test - Determining compressive strength of masonry units, Australian Standard, Sydney, Australia 2003.
[100] Correia AA, Tomassetti U, Costa AC, Penna A, Magenes G, Graziotti F. Collapse shake-table test on a URM-timber roof strucrure. In: 16th Eur. Conf. Earthq. Eng.; 2018. p. 1–12.
[101] Kallioras S, Guerrini G, Tomassetti U, Marchesi B, Penna A, Graziotti F, et al. Experimental seismic performance of a full-scale unreinforced clay-masonry building with flexible timber diaphragms. Eng Struct 2018;161:231–49. https://doi.org/10.1016/j.engstruct.2018.02.016.
[102] Kallioras S, Correia AA, Graziotti F, Penna A, Magenes G. Collapse shake-table testing of a clay-URM building with chimneys. Bull Earthq Eng 2019. https://doi.org/10.1007/s10518-019-00730-0.
[103] Almesfer N, Dizhur DY, Lumantarna R, Ingham JM. Material properties of existing unreinforced clay brick masonry buildings in New Zealand. Bull New Zeal Soc Earthq Eng 2014;47:75–96. https://doi.org/10.5459/bnzsee.47.2.75-96.
[104] EN 1052-3. Methods of test for masonry – Part 3: Determination of initial shear strength. Brussels, Belgium: European Standards, CEN/TC; 2002.
[105] ASTM. C1531. Standard test methods for in-situ measurement of masonry mortar joint shear strength index. West Conshohocken, PA: ASTM International; 2016.
[106] MS,. D6 In situ measurement of masonry bed joint shear strength. RILEM Recomm. Test. Use Constr. Mater., E & FN SPON 1996:470/475.
[107] Crowley H, Pinho R. Revisiting Eurocode 8 formulae for periods of vibration and their employment in linear seismic analysis. Earthq Eng Struct Dyn 2009. https://doi.org/10.1002/eqe.949.
[108] Leissa AW. Vibration of plates. Washington, DC, United States: 1969.
[109] Janich R. Die Näherungsweise Berechnung Der Eigenfrequenzen VonRechteckigen Platten Bei Verschiedenen Randbedingungen. Die Bautechnik 1962;3:93–9.
[110] Warburton GB. The vibration of rectangular plates. Proc Inst Mech Eng 1954;168:371–84. https://doi.org/10.1243/PIME_PROC_1954_168_040_02.
[111] EN 1052-1. Methods of test for masonry – Part 1: Determination of compressive strength. Brussels, Belgium: European Standards, CEN/TC; 1998.
[112] ASTM C1314. Standard Test Method for Compressive Strength of Masonry Prisms, West Conshohocken, PA, USA: ASTM Standard, ASTM International; 2018.
[113] Tondelli M, Beyer K, Dejong M. Influence of boundary conditions on the out-of-plane response of brick masonry walls in buildings with RC slabs. Earthq Eng Struct Dyn 2016. https://doi.org/10.1002/eqe.2710.
[114] Sharma S, Grottoli L, Tomassetti U, Graziotti F. Dataset from shake-table testing of four full-scale URM walls in a two-way bending configuration subjected to combined out-of-plane horizontal and vertical excitation. Data Br 2020;31:105851. https://doi.org/10.1016/j.dib.2020.105851.